DRAWDOWN PATTERNS RESULTING FROM PUMPING WELLS IN LEAKY PERCHED AQUIFERS

by

Catherine J. Goetz

Submitted in Partial Fulfillment of the Requirements for the Degree

Masters of Science in Hydrology

New Mexico Institute of Mining and Technology

Socorro, New Mexico

December 2010

ABSTRACT

This study explores the hydraulic response to pumping of leaky perched aquifers that receive continuous recharge. We explore whether distinct drawdown curves result that might reveal boundary effects or the position of the production well within the aquifer. Three-dimensional saturated-unsaturated simulations were developed to generate both circular (point-source recharge) and rectangular (line-source recharge) perched aquifer systems. Once the simulations stabilized at quasi steady-state in response to recharge, pumping at a constant-rate was imposed on the perched aquifer system. Diagnostic plots of the simulated log drawdown\ log time, as well as time-derivative curves, were analyzed. Results showed a repeatable, distinctive pattern of late-time negative slope-derivative curves that result from the size of the perched aquifer decreasing due to pumping and from continuing leakage through the aquitard as the system returns to steady-state. Because leakage decreases as the size and saturated thickness of the perched aquifer diminishes, additional water is available to meet pump demands and the rate of drawdown in the well decreases. This behavior is due to the small and constrained geometry of the aquifer. A lower pump rate required less reduction in aquifer size for the system to return to equilibrium, therefore, the appearance of the negative slope-derivative curve developed sooner than for simulations at higher pumping rates. Surprisingly, aquifer boundary effects were not readily apparent. Specific patterns

did not emerge to indicate the well location or perched-aquifer geometry. The simulated drawdown curves were also used to develop a methodology for obtaining transmissivity using the Copper-Jacob straight-line analysis.

Keywords: perched aquifer; drawdown; derivative curve; low transmissivity; MODFLOW-SURFACT; Aqtesolv.

TABLE OF CONTENTS

LIST OF FIGURES

LIST OF TABLES

ACKNOWLEDGEMENTS

I am grateful to my committee members Mike Fort, Dr. Mark Person (advisor), and Dr. Fred Phillips whose insights and suggestions furthered my education through the successful completion of this study. I wish to extend a special thanks to Mike Fort, who as an alumnus of Tech donated many hours of his time and expertise. Finally I wish to thank Dr. John Wilson who provided the genesis of this project.

DEDICATION

Although a small token, this thesis is dedicated to my husband Miles Diller. Returning to school, I left my career that I enjoyed as a geologist, moved to Socorro and commuted home on the weekends just because I was curious about hydrogeology. I have good reason to ask myself "what was I thinking?" I do not know. But I do know that through all this, Miles has been supportive and is deserving of more than a dedication in a thesis that sits on a library shelf collecting dust.

This thesis is accepted on behalf of the

Faculty of the Institute by the following committee:

_____

Advisor

_____

_____

_____

Date

I release this document to the New Mexico Institute of Mining and Technology.

_____

Student's Signature Date

CHAPTER 1 - INTRODUCTION

Perched aquifers are unconfined water-bearing units within the vadose zone. These aquifers, which are of limited areal extent, typically develop from surface water sources (e.g., ponds or streams) infiltrating through the vadose zone, accumulating on a layer of less permeable lithology (Figure 1-1) (Fetter 1994).

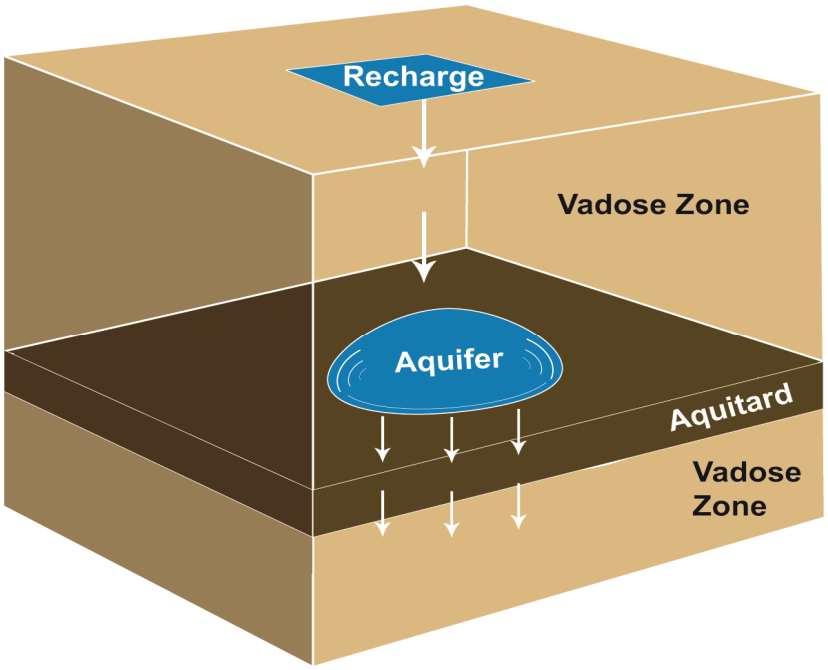

Figure 1-1. Schematic diagram showing a perched aquifer formed on a leaky aquitard.

Perched aquifers are of little importance for municipal water supply but may contribute to contaminant transport, particularly if the recharge source is an industrial discharge pond or stream receiving untreated effluents (Hueni 2010). Investigation of potentially contaminated sites often involves the drilling, installation, and subsequent testing of monitoring wells to determine the aquifer transmissivity and storage parameters (Hall 1996). These properties can be obtained using single-well aquifer test methods (Driscoll 1986). During these tests the well drawdown is measured over time while pump discharge is maintained constant. The resulting drawdown curve is evaluated using analytical solutions and their associated graphical depictions to estimate the aquifer parameters (Schwartz et al. 2003). These solutions assume an unconfined aquifer of infinite radial extent, ignoring the boundary effects of the perched system. If a constant-rate pump test could also determine properties unique to a perched aquifer (e.g., distance to a perched aquifer boundary) this would be of benefit to remediation strategies.

Previous perched-aquifer research has largely focused on the role of these water-bearing units as a component of local or regional groundwater investigations. The application of these studies is varied, reflecting the participation of perched aquifers in diverse aspects of groundwater functions. Rains et al. (2006) showed the relationship of perched aquifers to certain wetland ecosystems by evaluating the connectivity of perched systems to vernal pools. Wu et al. (1999) investigated the effect of perched aquifers in construction and waste applications by exploring their occurrence and lateral groundwater flow at a proposed subsurface waste repository. Other studies investigated the role of perched aquifers as a groundwater migration pathway for potential contaminants. These investigations typically focused on the presence or absence of

contaminants in perched units and the connectivity of these units within the local or regional groundwater system. A range of contaminants occurring in perched aquifers have been examined including sea water, petroleum contaminants, pesticides, etc. (Reichard et al. 1995, Cozzarelli et al. 1999, Behaera et al. 2003).

Mathematical descriptions have been generated for perched aquifers serving as subsurface water storage reservoirs. Bouwer et al. (1999) presented a solution for predicting the height of a perched aquifer subjected to artificial recharge, while Anakhaev (2009) examined a similar subsurface feature by obtaining a steady-state flow solution for a perched mound. Previous research has also explored the formation of perched aquifers given certain structural features. Bagtzoglou (2003) investigated the mechanisms for the genesis of perched water in fault systems and the recharge rates required to sustain the system.

While there are numerous studies on perched aquifers as a component of local or regional groundwater systems, analytical solutions describing the behavior of a perched aquifer are few in number with little analysis on the hydraulic response of a perched aquifer to perturbations. Therefore, conventional analysis of constant-rate pump tests conducted on perched systems is chiefly based on solutions formulated for infinite-in-extent unconfined aquifers. These solutions include the delayed-yield solution first developed by Boulton (1954) and expanded upon by numerous researchers (e.g. Neuman 1972, 1974; Moench 1995). The analytical solutions may provide insights into aspects of the unconfined behavior of perched aquifers. However, they do not address several important attributes of perched aquifers including their limited spatial extent and variable thickness.

Mathematical advances in describing the perched aquifer response to perturbations is largely a product of unconfined flow studies having components relevant to perched systems. For example, Serrano (2003) presents a model for groundwater flow experiencing a nonlinear moving boundary with vertical flow that was field-verified on a perched aquifer with periodic recharge. Although the development of analytical solutions and numerical models representing the nonlinear behavior associated with perched aquifers (vertical flow, moving phreatic surface of variable thickness) presents challenges, it has been suggested that the lack of literature in this area likely reflects a focus on groundwater supply development thereby leaving perched aquifer hydrology "an unexplored frontier" (Fogg 2003).

This study is perhaps the first to explore the hydrologic response of a leaky perched aquifer to constant pumping. The goal is to ascertain whether distinctive drawdown curves result that could enable the unit's limited extent and geometry to be defined, as well as the position of the well within the aquifer. To achieve this, three-dimensional simulations using MODFLOW-SURFACT (HydroGeoLogic, Inc. 2007) were developed to generate perched aquifers and subsequently perform the constant-rate pump tests. The pump test results were analyzed using Aqtesolv (Duffield 2007) to generate drawdown and time-derivative curves for aquifer behavior analysis. The time-derivative curve is calculated as the derivative of drawdown with respect to the natural logarithm of time and will be referred to as the derivative curve in this study.

As the drawdown pattern from a constant-rate pump test conducted on a leaky perched aquifer was unknown, an initial review of existing analytical solutions was instructive. The Theis solution (1935) for a confined aquifer of infinite lateral extent

serves as a guide to ideal confined aquifer behavior, while additional analytical solutions describe particular components of the leaky perched-aquifer system. Specifically, the drawdown and derivative curves from the leaky perched aquifer were compared to analytical solutions of the flow equations for three sets of aquifer boundary conditions: unconfined aquifer with instantaneous delayed yield, leaky aquitard, and no-flow lateral boundary (Figure 1-2). We hypothesized that drawdown patterns from an aquifer test conducted in a leaky perched aquifer could exhibit some or all of these features. Neuman (1972) solved the flow equation for a laterally infinite unconfined aquifer with instantaneous delayed gravity drainage, also referred to as delayed yield. The time-drawdown curve produces an “S” shape reflecting the early time response to elastic storage, intermediate time contribution from delayed gravity drainage of water from the pores within the cone of depression, and late time radial flow of the infinite-acting aquifer (Figure 1-2 a). (Schwartz et al. 2003). The derivative curve identifies the delayed yield by a "V" shape while the late time, infinite-acting radial flow is a horizontal line (Renard et al. 2009). Figure 1-2 (a) presents an example of the drawdown and derivative curves depicting the pattern that results from delayed yield in an infinite aquifer. A schematic of this idealized aquifer scenario is also shown.

A second component of time-drawdown response to pumping that may be found in the perched-aquifer scenario is the effect of a leaky aquitard (Figure 1-2 b). The analytical solution for pumping of a confined aquifer with an overlying leaky aquitard and unconfined aquifer was developed by Hantush and Jacob (1955). Leakage across a semi-permeable confining unit provides an additional supply of water to the confined aquifer, resulting in less drawdown at late time than would be predicted from the Theis

solution (Figure 1-2 b). The derivative curve reflects this; the rate of drawdown in the well decreases at intermediate time and the slope of the derivative becomes negative, dropping to zero when the drawdown stabilizes at late time (Figure 1-2 b). For a perched aquifer, the leakage is downward out of the aquifer, diminishing as the head declines due to pumping.

A third hydrologic response considered in this study is the impact due to boundaries (in our case, the edge of the perched aquifer). Image well theory is often utilized to determine drawdown response to boundaries by mimicking a physical barrier using superposition theory. The effects of an imaginary or "image well" are added to the predicted drawdown from the "real" well. Where the cone of depressions of the real and image wells overlap, the drawdowns are added (Ferris et al. 1962). Encountering an impermeable boundary has the effect of increasing (doubling) the drawdown predicted by the Theis solution at the boundary. Figure 1-2(c) depicts the increase in slope in the drawdown and derivative curves in a confined aquifer pump test when an infinite linear impermeable boundary is encountered (Renard et al. 2009). A perched aquifer is bounded by the locus of positions at which the saturated thickness goes to zero. While application of the method of images to unconfined aquifers with variable saturated thickness is not strictly applicable, analogous results of positive slope drawdown and derivative curves were observed in verification tests on unconfined aquifers of uniform thickness where drawdown encountered model no-flow boundaries (Appendix A) (Schwartz et al. 2003). Additional techniques in reservoir test analysis use diagnostic plots and tools to describe flow systems deviating from infinite-in-extent models (Bourdet et al. 1989, Cinco-Ley et al. 1981, Barker 1988). The methods describe flow regimes having limited boundaries

that also depict diagnostic derivative plots of increasing slopes. While these are typically applied to fracture-flow analysis in the petroleum industry, application of these techniques to hydrogeological problems is valid and appropriate (Walker et al. 2003, Renard et al. 2009). The drawdown curve response to these three cases of aquifer behavior - unconfined with instantaneous delayed yield, leaky, and boundaries - serve to facilitate evaluations of the simulated constant-rate pump tests of the leaky perched aquifer by either presence or absence and sequence of these features in test results. Using these identified patterns as well as unanticipated responses, the drawdown and derivative curves were analyzed to determine if constant-rate pump tests could be used to identify a perched aquifer as limited in extent, or to identify it as of a particular geometry, or to determine the well position within the perched aquifer.

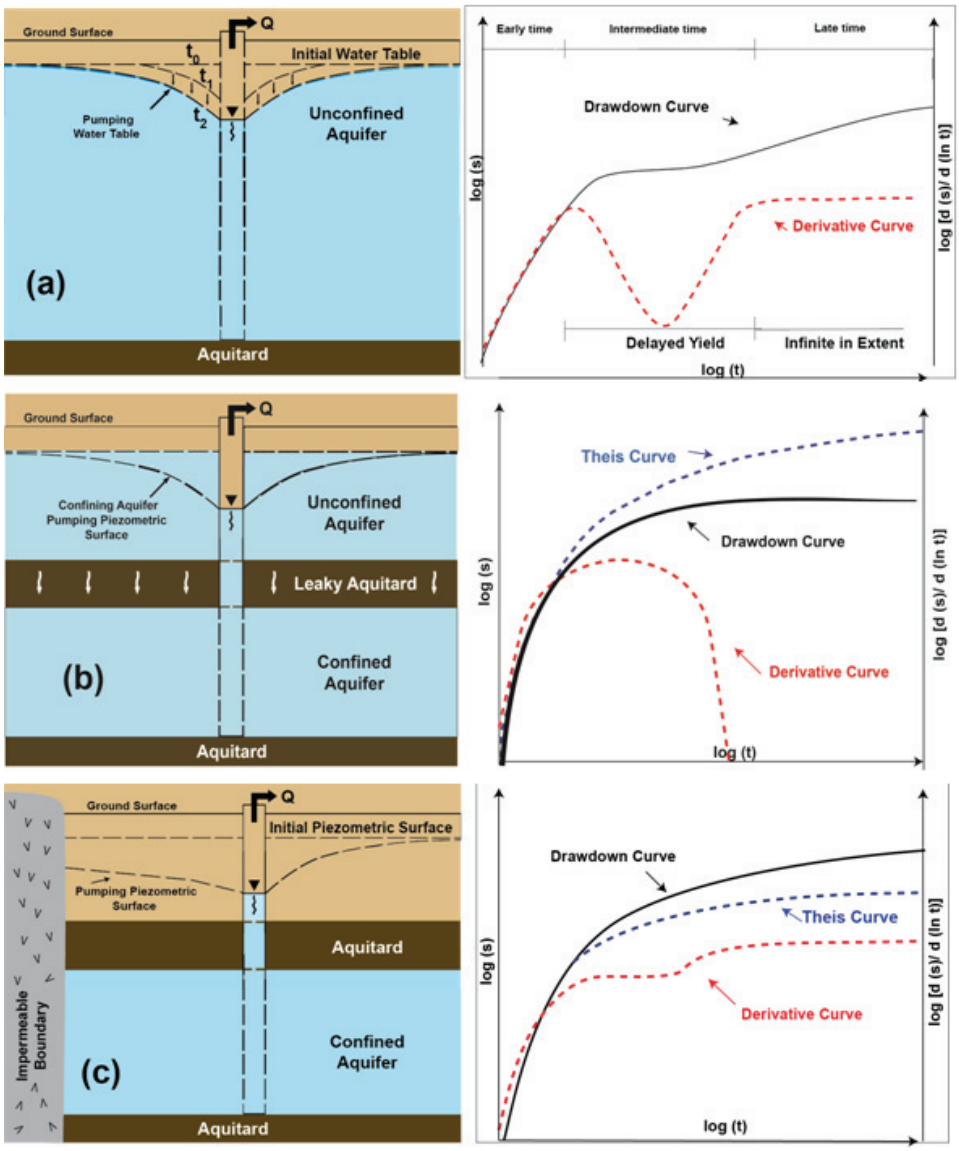

Figure 1-2. Schematic diagrams of aquifers and respective drawdown (black) and derivative (red) curves: (a) unconfined with instantaneous delayed gravity drainage, (b) leaky confined, (c) confined with impermeable boundary. Variables used: are s, drawdown; t, time; and, d, derivative.

In the remainder of this manuscript, we describe the perched aquifer conceptual models used in this study (Chapter 2). The methods and software used, including the governing equation used in MODFLOW-SURFACT, are described in Chapter 3 with the

numerical grids constructed for the pond and stream based recharge scenarios following in Chapter 4. We then present simulation results (Chapter 5) followed by the discussion of findings and concluding remarks (Chapter 6). Appendix A contains the results of software verification testing and Appendix B presents additional models of infinite-in-extent unconfined aquifers to assist in the perched aquifer drawdown curve analyses.

The simulations were conducted in the United States Customary System or English measurement units. The use of the English system facilitated refined discretization conducted on test models. The following table (Table 1-1) provides conversion to many common values used in this study.

Parameter	English	International System of Units
Length	1 foot (ft)	0.3048 meters (m)
Area	1 square foot (ft^2)	0.0929 square meters (m^2)
Volume	1 cubic foot (ft^3)	0.0283 cubic meter (m^3)
Hydraulic Conductivity	1 foot/day (ft/day)	3.528E-6 meter/second (m/s)
Transmissivity	1 square foot/day (ft^2/day)	1.075E-6 square meters/second (m^2/s)
Flow Rate	1 cubic foot/day (ft^3/day)	3.277E-7 cubic meter/second (m^3/s)

Table 1-1. Conversion of English to International System of Units for parameters used in this study.

CHAPTER 2 - CONCEPTUAL MODEL

Our conceptual model of a perched aquifer system used in this study consists of a thick vadose zone bounded at the base by a less permeable, leaky aquitard of continuous lateral extent and finite thickness. Below the base of the aquitard was a thick unsaturated layer having the same properties as the upper vadose zone. All hydrostratigraphic units were modeled as isotropic and homogenous. Recharge was applied over a portion of the top surface, infiltrating through the vadose zone and accumulating on the top of the aquitard to form a perched aquifer. This zone of enhanced recharge could represent surface water sources such as a pond, stream, or impoundment. Quasi steady-state conditions for the perched aquifer were assumed. We required that the total recharge entering the system equaled the total volume of water leaking through the aquitard. Note that the footprint of the perched aquifer was less than the lateral extent of the aquitard. Two perched aquifer shapes were examined. First, a circular aquifer resulting from a small square recharge area was considered. This recharge geometry is intended to replicate discharge from a pond or impoundment. Second, a rectangular aquifer formed by a thin rectangular recharge area extending across the model was examined. This recharge geometry is intended to represent infiltration from a stream or river (Figure 2-1).

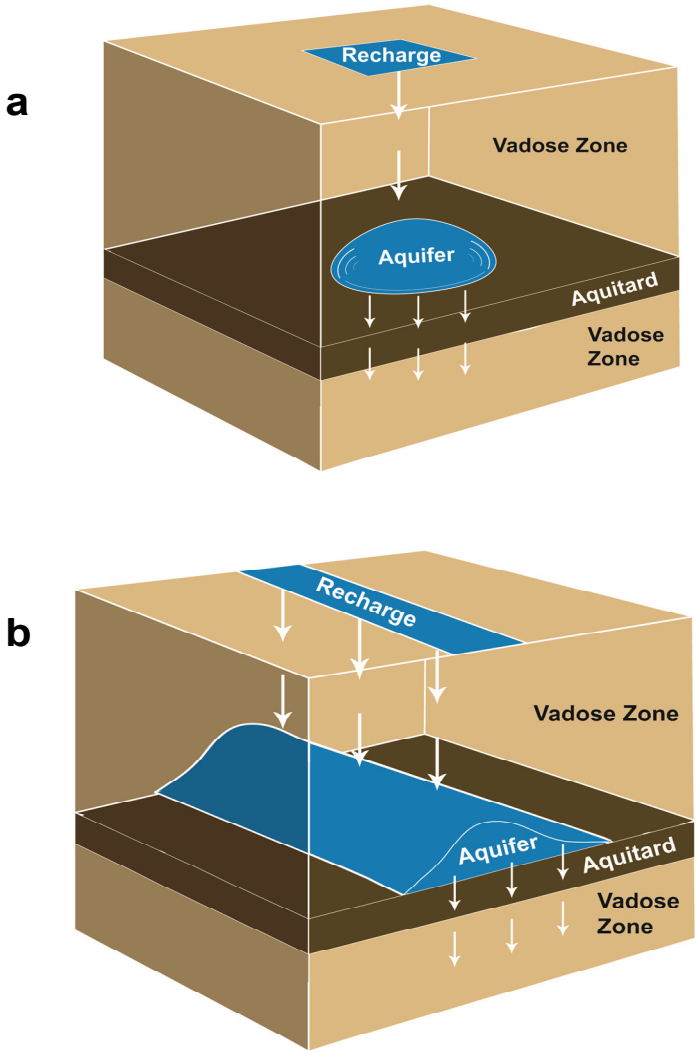

Figure 2-1. Schematic diagrams illustrating (a) Circular and (b) Rectangular Aquifer Conceptual Models.

Following perched-aquifer development for these two scenarios, a constant-rate pump test was conducted using a fully penetrating extraction well. Once extraction began, the system shifted from steady-state to transient conditions. To replicate field operations where observation wells may be lacking, drawdown data was collected from the extraction well. The extraction well was placed in differing locations within each

aquifer shape to assess the effect of well placement on drawdown curves. The circular aquifer was evaluated in three locations: center, off-center, and edge. The rectangular aquifer was examined in two locations: center and edge. In addition to various well placements, each shape was assessed using two differing aquifer hydraulic conductivities (K), 0.2 ft/day and 3.0 ft/day. Recharge rates required pairing to appropriate hydraulic conductivities of the aquifer (K) with those of the aquitard (K') so as to produce a sufficient saturated thickness to enable a pump test to be conducted and also to prevent the lateral spreading of the growing aquifer from encountering the boundaries of the modeled flow domain before steady-state conditions were reached. The lower hydraulic conductivity (0.2 ft/day) supported perched-aquifer growth at a low recharge rate (5.5E-3 ft^3/day) over a relatively long duration (approximately 550 years), intended to be comparable to typical natural conditions, while the higher hydraulic conductivity required an intense (0.25 ft^3/day), short-duration (approximately 5.5 years) recharge event that could simulate anthropogenic releases.

CHAPTER 3 - METHOD

Modeling Software

Because multiple processes (leakage, delayed yield, boundary effects) can all interact simultaneously while pumping a perched aquifer, we utilized numerical modeling in this study. The governing equation describing saturated-unsaturated flow through the vadose zone used in this study is given by:

$$\frac{\partial}{\partial x}\left[K_{xx}k_{rw}\frac{\partial h}{\partial x}\right]+\frac{\partial}{\partial y}\left[K_{yy}k_{rw}\frac{\partial h}{\partial y}\right]+\frac{\partial}{\partial z}\left[K_{zz}k_{rw}\frac{\partial h}{\partial z}\right]-W=\phi\frac{\partial S_w}{\partial t}+S_wS_s\frac{\partial h}{\partial t} \qquad (1)$$

Where K_{xx}, K_{yy}, K_{zz} is saturated hydraulic conductivity in the principal directions (ft/day), k_{rw} is relative permeability (unitless), h is hydraulic head (ft), W is sources or sinks (ft^3/day), ϕ is drainable porosity or specific yield (Sy) (unitless), S_w is degree of saturation (unitless), and S_s is specific storage (1/ft) (HydroGeoLogic, Inc. 2007).

This equation was solved numerically using the block-centered finite-difference groundwater flow-modeling package MODFLOW-SURFACT. MODFLOW-SURFACT is a commercial software package developed by HydroGeoLogic, Inc. (2007), with the pre- and post-processor Visual MODFLOW (Schlumberger 2009). Input data formats for MODFLOW-SURFACT are based on the commonly used saturated zone finite-difference method groundwater model named the United States Geological Survey (USGS) Modular Flow Model (MODFLOW) (McDonald and Harbaugh 1988).

MODFLOW-SURFACT provides additional capabilities to MODFLOW for unsaturated/saturated interactions and replication of well pumping which include the ability to simulate the vertical unsaturated/saturated sequences seen in perched aquifers, the use of well packages which permit the addition of wellbore storage and the apportioning of well withdrawal to well nodes, and a simplified approach (linearization) to the analysis of variably-saturated flow. This simplification utilizes pseudo-soil to define the relationship between pressure head and relative permeability and saturation to assess unconfined flow in lieu of soil type functions (e.g., van Genuchten functions) (HydroGeoLogic, Inc. 2007). Saturated/unsaturated flow is mathematically highly nonlinear. MODFLOW-SURFACT linearizes the degree of saturation, S_w, and thus relative permeability, $k_{rw,}$ in order to achieve high computational efficiency and mass conservation. The degree of saturation, which is a function of pressure head (ψ), is determined for a grid cell by assigning a value of 1 for cells with the hydraulic head above or at the elevation of the top of the cell and zero when the head is at or below the bottom elevation of the grid cell. Integrating vertically across the grid cell provides a straight line relationship, $S_w(\psi) = \overline{S_w}$. The dimensionless value for $\overline{S_w}$ ranges between 0 and 1. Relative permeability, k_{rw}, depends on the degree of saturation of the cell. Therefore, setting $k_{rw} = \overline{S_w}$ further reduces the complexity of the nonlinear variably saturated flow equation (Panday et al. 2008). While these functional relationships lack the specificity of soil type functions, they provided a computationally efficient means to assess the variably saturated flow.

After completing the pump-test simulations, drawdown data was exported from MODFLOW-SURFACT and imported into Aqtesolv (Duffield 2007). Two graphical

depictions of the aquifer test were generated for each simulation: the drawdown curve, representing either the log or linear drawdown versus log time, and the time-derivative curve. The time-derivative of the drawdown is referred to as the derivative curve in this study and as is computed by:

$$\frac{ds}{d\ln(t)}i = \frac{\left[\frac{\Delta s_1}{\Delta \ln(t_1)}\Delta \ln(t_2) + \frac{\Delta s_2}{\Delta \ln(t_2)}\Delta \ln(t_1)\right]}{\left[\Delta \ln(t_1) + \Delta \ln(t_2)\right]} \quad (2)$$

Where i is the point of interest on the drawdown curve, s is drawdown, and t is time (Duffield 2007). The method was presented by Bourdet et al. (1989) as a preferred approach to calculating the derivative due to its accuracy over the duration of the test. Noise reduction in the derivative curve is implemented using the Bourdet method where the distance between the points of interest is determined by a variable, L, that specifies the separation between the points of interest according to the fraction of log cycle. Values of L generally range from 0.1 to 0.5 log cycles, where 0.5 would be considered in severe cases (Bourdet et al. 1989). Figures of the drawdown and derivative curves presented in this study were generated using Aqtesolv.

Verification Testing of Software

The MODFLOW-SURFACT simulations and Aqtesolv drawdown and derivative-curve analyses were verified for the ability to reproduce predicted parameters and response to boundaries using simple simulations of constant-rate pump tests (Appendix A). The verification simulations consisted of square models of various dimensions pumped by wells fully penetrating homogenous, isotropic media of uniform aquifer thickness, bounded by no-flow boundaries. These verification models were run using

different grid discretizations to compare the shape of the resultant drawdown curves. The models produce similar curve shapes for all grid sizes. As the purpose of the study was to assess the drawdown data collected from the extraction well rather than observation wells, the verification tests analyzed the pumping well drawdown data. Results of these tests show that computed values for transmissivity were comparable to input values, but the calculated storage coefficient values varied due to the limitations of collecting data from the extraction well (e.g. wellbore storage effects). Additional models of limited extent were used to confirm predicted response to boundaries (Appendix A).

CHAPTER 4 - NUMERICAL MODELS

Circular Perched Aquifer Model

The grid dimensions of the circular perched-aquifer model were 2000 ft in length (L) by 2000 ft in width (W) by 300 ft in height (H). The elevation of the top of the solution domain was set at 300 ft. Two vadose-zone hydraulic conductivities were tested. A relatively low saturated hydraulic conductivity of 0.2 ft/day model was discretized using 89 rows, 89 columns, and 44 layers. The saturated hydraulic conductivity for the aquitard in this model was 1E-5 ft/day. Additional simulations were conducted using a model of higher hydraulic conductivities, 3.0 ft/day for the vadose zone and 0.003 ft/day for the aquitard. The solution domain for the high hydraulic conductivity scenario was discretized using 108 rows, 108 columns, and 48 layers. For both models, the lateral grid spacing was approximately 5 ft in the region of the pumping well with spacing increasing outward. Vertical grid refinement was concentrated in the region above the aquitard in the perched-aquifer zone. Here, grid refinement was approximately 2.5 ft thick with resolution increasing in the z- direction below the aquitard and at the upper surface of the model to a maximum of 10 ft thick. Adjustments in the grid spacing were made to ensure the accuracy of two simulations of the higher-hydraulic-conductivity scenario. In one instance using a pump rate of 1000 ft^3/day and a center well location, the smallest grid

size was increased to 10 ft to prevent early dewatering of the wellbore. In the other case using an edge well, the smallest grid was reduced to 2.5 ft to improve the quality of the resulting drawdown curve.

The lateral boundaries of the flow domain were set as no-flow boundaries. The lowermost layer of the model was a constant head/water table layer ($\psi \approx 0$) that served to remove downward leakage from the simulation domain. The uppermost layer of the model contained a 100 ft (L) by 100 ft (W) recharge area where a constant flux was prescribed. The remaining cells were set at zero head for the (hydrostatic) initial condition in generating the perched aquifer. The aquitard was 20 ft thick and located approximately 200 ft below the surface. Specific yield and effective porosity were 0.3, total porosity was 0.35. Table 4-1 presents the remaining model parameters and resulting steady-state circular aquifer dimensions.

Aquifer Scenario	Aquifer K (ft/day)	Aquitard K' (ft/day)	S_s (1/ft)	Recharge Rate (ft^3/day)	Recharge Zone (L x W) (ft x ft)	Total Recharge (ft^3/day)	Days to Steady-State (days)	Steady-State Size (W x H) (ft)
Circular	0.2	1E-5	3E-5	5.5E-3	100 x 100	55	200,000	1117 x 14.4
	3.0	3E-3	6E-6	0.25	100 x 100	2500	2,000	539 x 20.8
Rectangular	0.2	1E-4	3E-5	5.5E-3	1500 x 40	330	200,000	600 x 12.4
	3.0	3E-3	6E-6	0.25	1500 x 20	7500	4,000	438 x 13.7

Table 4-1. Circular and Rectangular Aquifer Parameters.

The model was initialized with a zero hydrostatic head, after which a specified recharge was applied to the model upper boundary. Durations to achieve quasi steady-state are shown in Table 4-1. The steady-state head values were then imported into a second identical model augmented with a fully penetrating pumping well to simulate constant-rate pump tests. Various pump rates and well locations were used in the simulations to assess the impact on well drawdown. Depending on the saturated hydraulic conductivity used in a given simulation, the extraction rates and test durations were varied to prevent rapid dewatering of the wellbore and to allow sufficient time for aquifer response. Figure 4-1(a) represents the generalized footprint of the circular perched-

aquifer model and identifies the well locations and outline of the surface recharge area. As the simulations from the two aquifer hydraulic conductivities tested produced different sized aquifers, the figure is not to scale. The points A and A' indicate the position of cross sections in the following chapter. The pump rates for the various well locations are found in Table 4-2.

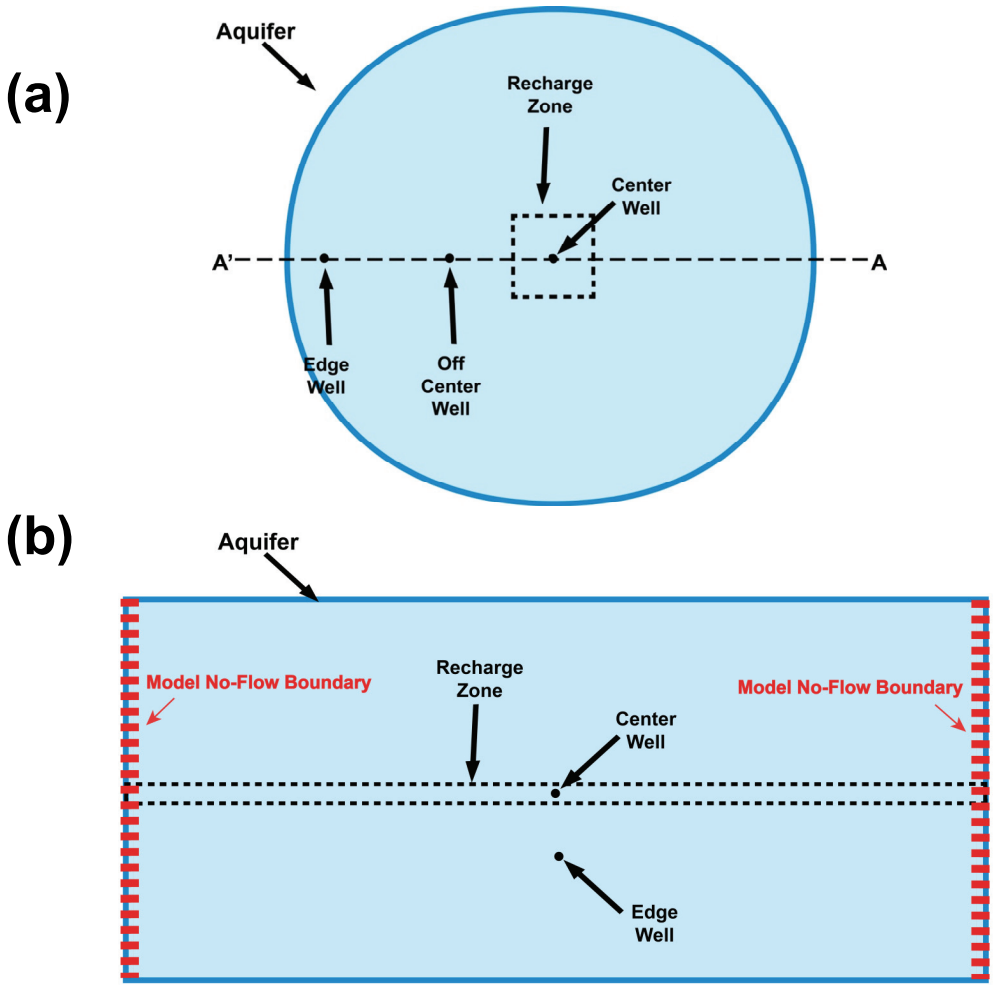

Figure 4-1. Footprint of circular (a), and rectangular (b) aquifers with relative well locations. The rectangular perched aquifer represents a section of an infinite-in-extent stream recharge source. A- A' denotes location of the circular aquifer cross sections presented in the following chapter.

Aquifer scenario	Aquifer K (ft/day)	Well Location	Pump Rates (ft^3/day)	Duration of Test (days)
Circular	0.2	Center	10, 25	10, 000
		Off-Center	10	10, 000
		Edge	2	10, 000
	3.0	Center	50, 100, 600, 1000	1,000
		Off-Center	50, 100, 300	1,000
		Edge	10, 40	1,000
Rectangular	0.2	Center	10	10,000
		Off-Center	2	10,000
	3.0	Center	100, 300	1,000
		Off-Center	100	1,000

Table 4-2. Circular and Rectangular Aquifer Pump Rates.

Rectangular Perched Aquifer Model

For both hydraulic conductivity scenarios, the rectangular perched aquifer model dimensions were 1500 ft (W) by 5000 ft (L) by 300 ft (H) comprising 54 rows, 100 columns, and 46 layers. The grid cell size was smallest in the region of the pumping well (10 ft), coarsening outward to the model boundaries to a maximum cell size of approximately 80 ft. Vertical layers vary from 2.5 ft in the region of perched aquifer development to 10 ft in the overlying vadose zone. The aquitard was 20 ft thick, located 240 ft below the top surface. The model side boundaries were no-flow boundaries. The

lowermost layer of the model was a constant head layer to remove excess leakage. Recharge was applied to the surface as a strip extending the length of the model and along the centerline of the width (Figure 4-1b). The remaining cells were zero head for the initial conditions of the simulations for perched aquifer development. The Sy, Ss, effective porosity, and porosity were the same as for the circular models. The remaining parameters and resulting perched-aquifer dimensions are presented in Table 4-1. As in the circular perched-aquifer scenario, the steady-state head values from the rectangular aquifer generation models were imported into a second identical model for constant-rate pump-test simulations. Figure 4-2 shows the generalized rectangular perched-aquifer footprint, recharge zone, and well locations. The corresponding pump rates are found in Table 4-2.

CHAPTER 5 - RESULTS

Circular Perched Aquifer

Model Initialization

Starting from the hydrostatic initial conditions, the simulations were run for 5.5 years until quasi-steady state conditions were achieved. The aquifer and aquitard parameters as well as recharge conditions are listed in Table 4-1. The perched aquifer extent eventually stabilized due to the increases in basal leakage out the bottom of the relatively low-permeability aquitard. The perched aquifer had a parabolic shape over the recharge area and a linear profile elsewhere. Figure 5-1 shows the cross section through the center of the aquifer as extraction began with 1x and 5x vertical exaggeration. The 5x vertical exaggeration is used in the remainder of the document in order to enable the flow regime to be shown at a fine scale. Groundwater flow directions in response to recharge are indicated by the arrows. Note that the shaft lengths in Figure 5-1 do not reflect groundwater flow rates. For the permeability and recharge rates used, the perched aquifer had an aspect ratio representing the length to the height of the perched aquifer of about 10:1.

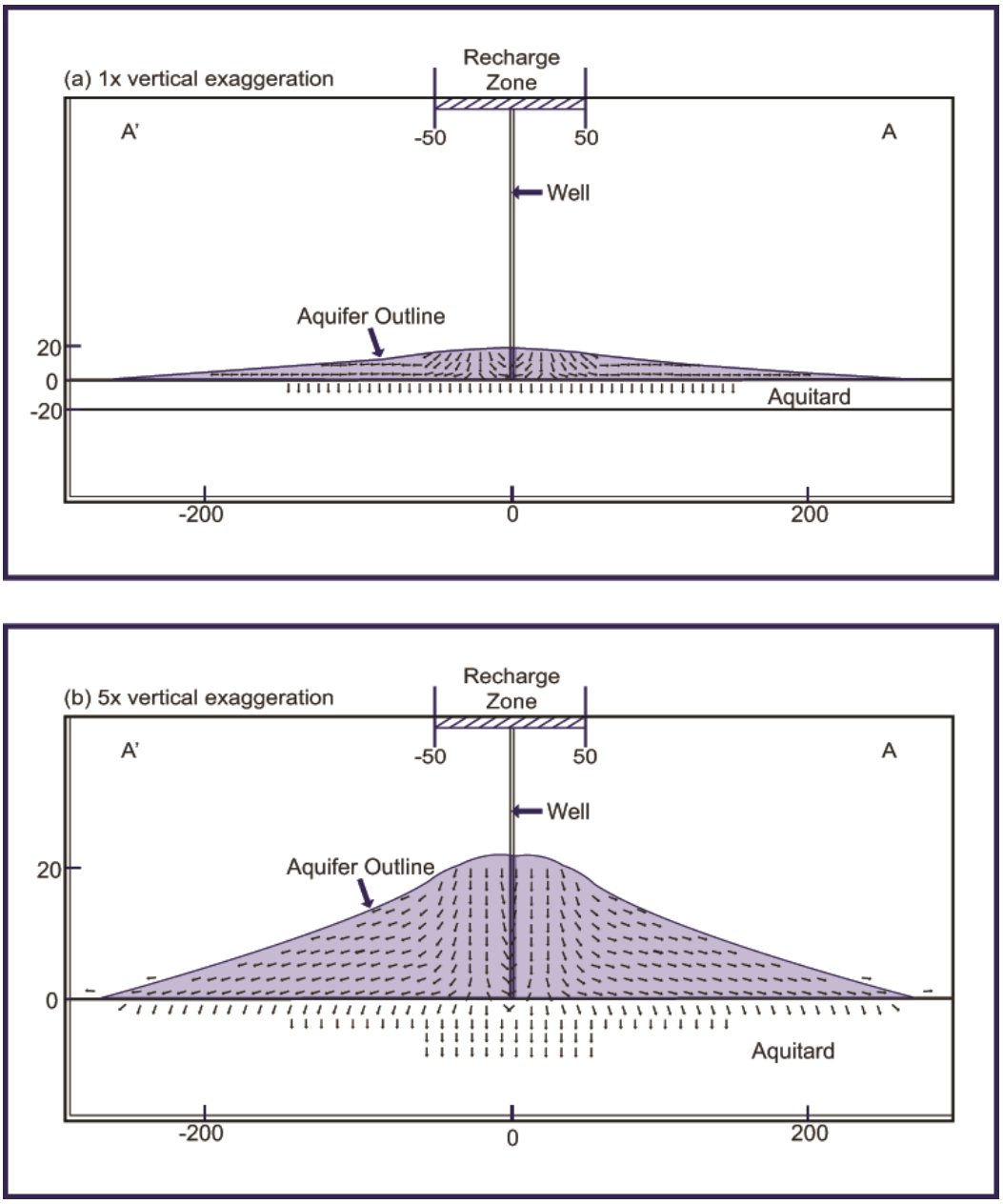

Figure 5-1. Cross section through the center of the circular model at initial time for the 600 ft^3/day pump rate test with no vertical exaggeration (a) and 5x vertical exaggeration (b). Small arrows indicate flow direction. Shaft lengths do not represent flow rates.

Center Well Location

Our analysis starts with the placement of a well in the center of the perched aquifer (Figure 5-2). The well was continuously pumped at a rate of 600 ft^3/day. This extraction rate is 25% of the total recharge rate. Pumping resulted in the development of a flow divide or capture zone moving inward to supply to the well and outward to sustain the aquifer flanks. Leakage into the aquitard was also observed. As pumping continued, the aquifer height decreased and the cone of depression became broader and deeper. The flow paths extended outward. The flow divide shifted outward, expanding the captured recharge to approximately 600 ft^3/day after 10 days (a capture zone radius of approximately 27.9 ft), sufficient to meet pump demands if leakage beneath this radius were not a factor. From 10 to 1,000 days, the capture zone radius increased to approximately 28.3 ft, equivalent to an estimated 630 ft^3/day captured recharge with approximately 30 ft^3/day of water leaking across the aquitard below. The "Final" line depicted in Figure 5-2 denotes the simulation at the completion of the constant-rate pump test (1,000 days). Also shown, is the outline of the aquifer at the initial time step to illustrate the decrease in aquifer size.

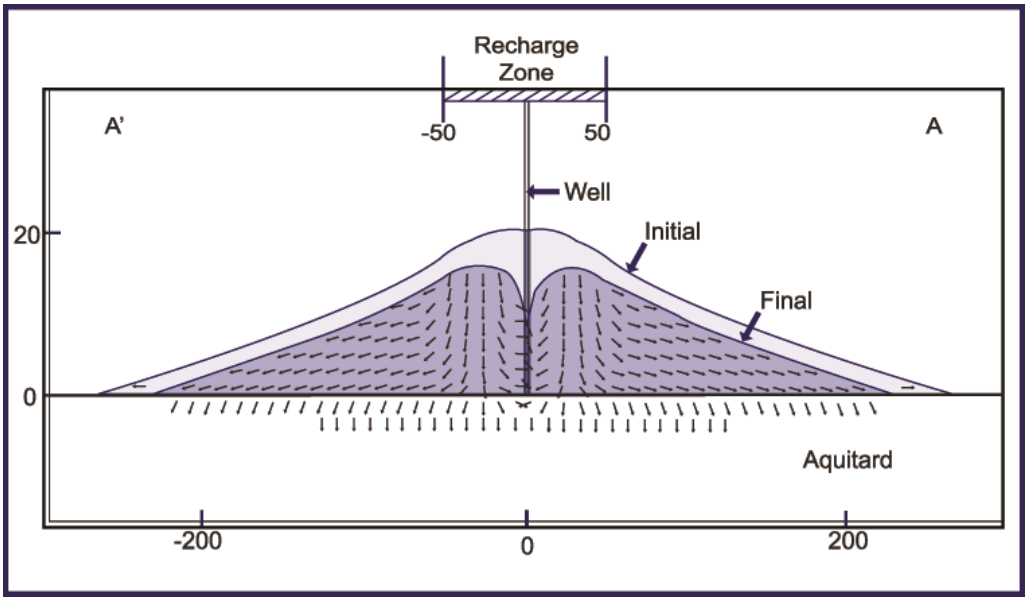

Figure 5-2. Cross section of the circular center well model conducted at 600 ft^3/day pump rate at 1,000 days, the test completion. Outline in background shows the initial shape of the aquifer.

The maximum aquifer height was lowered by approximately 4.8 ft during the test. Nearly 50% of the change in aquifer thickness occurs within the first 10 days. The aquifer size was further diminished by a decrease in the footprint radius of 40 ft by the completion of the test. The areal extent of the perched aquifer footprint decreased by 62,800 ft^2 which represents a 27% reduction from the original aquifer area.

The relationship between maximum aquifer height, reduction in footprint radius, reduction in total leakage rate, and well drawdown is presented in Figure 5-3. The parameters shown serve to track physical processes involved during the constant-rate pump test. The maximum aquifer height acts as a proxy for changes in transmissivity, storage, the available height to induce leakage, and gradient to the periphery of the

aquifer. As recharge and extraction rate were held constant, the changes in total leakage rate reveal the response to equilibrate sources and sinks.

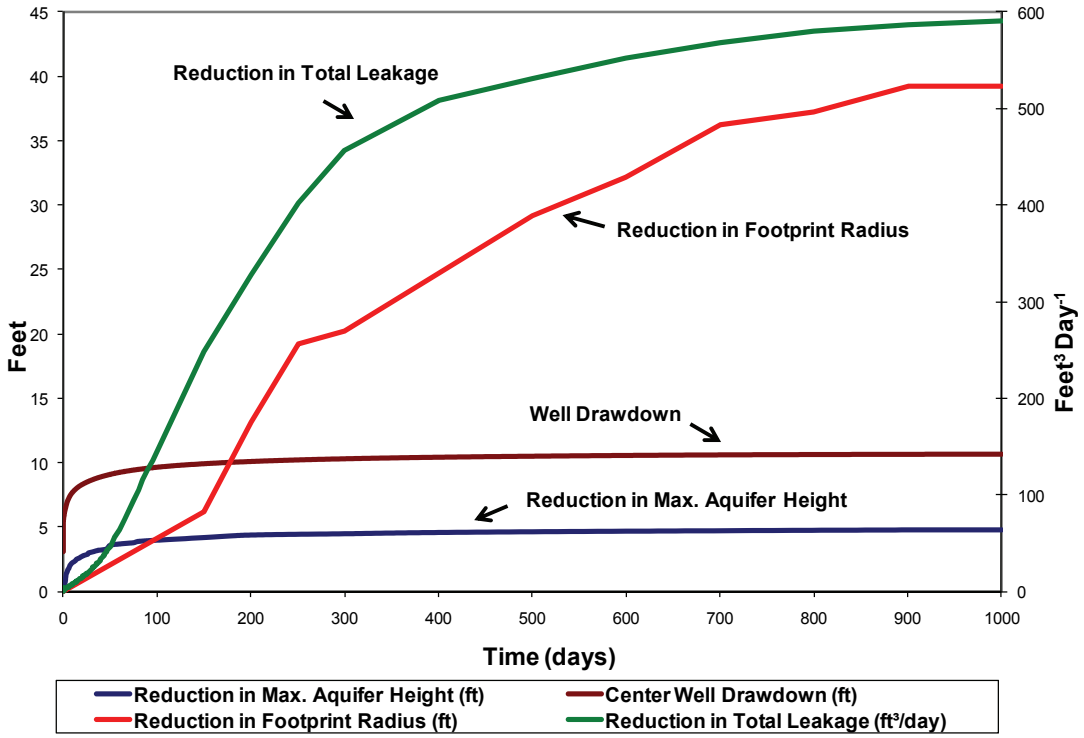

Figure 5-3. Changes in drawdown (brown line), total leakage (green line), aquifer height (blue line), and perched aquifer radius (red line) for the circular perched aquifer model. The production well was located at the center of the perched aquifer and pumped at a constant rate of 600 ft^3/day.

The decline in aquifer height and increase in drawdown largely occurred within the first 100 days. Drawdown in the well paralleled the reduction in aquifer height. It is after the early time period that both a reduction in the total leakage rate and footprint radius were prominent. The final total leakage rate was 1909 ft^3/day. As the pump rate was 600 ft^3/day, the total sinks to the system (leakage plus pump extraction) approaches

the total recharge rate (2500 ft^3/day). As seen in Figure 5-3, greater than 90% of the reduction in footprint area and height has occurred within 700 days of pumping which corresponds to the response time of the perched aquifer to changes in hydraulic stress (τ):

$$\tau = \frac{L^2 S_y}{T} = \frac{(270\,ft)^2 \cdot 0.3}{30\,\frac{ft^2}{day}} = 729\,\text{days} \qquad (3)$$

where T is average aquifer transmissivity (saturated thickness of 10 feet), Sy is specific yield, and L is the radius of the perched aquifer (Phillips 1991).

The response depicted in the Figures 5-1, 5-2, and 5-3 suggest that recharge and changes in aquifer storage met the initial extraction demand. As less recharge was available to sustain the aquifer due to pumping and leakage, the size of the aquifer diminished from a decrease in footprint and/or thickness. The reduced size of the aquifer decreased the total water loss leaked through the aquitard. Less leakage provided more recharge water to meet the pump demand. As the recharge supplied a greater component to the pump, the volume removed from aquifer storage decreased, effectively reducing the rate of drawdown in the well. A simplified approach to the sources and sinks, W, in the MODFLOW-SURFACT governing equation (Eq. 1) can be described as:

$$W = \text{Pumping (Q)} + \text{Leakage (L)} - \text{Recharge (R)}. \qquad (4)$$

The total recharge and pumping rate were held constant for each simulation. The total leakage rate is a function of perched aquifer saturated thickness (h) and area which is in turn a function of the radius of the perched aquifer (r). Thus, leakage (L) is a function of h, r. As the shape of the aquifer reduced, leakage decreased. For the system to return to steady-state, the size of the aquifer must decrease sufficiently to cause a reduction in total leakage rate equal to the pumping rate. The perched-aquifer response to

pumping as described above can be seen in the drawdown and derivative curves monitored within the production well (Figure 5-4).

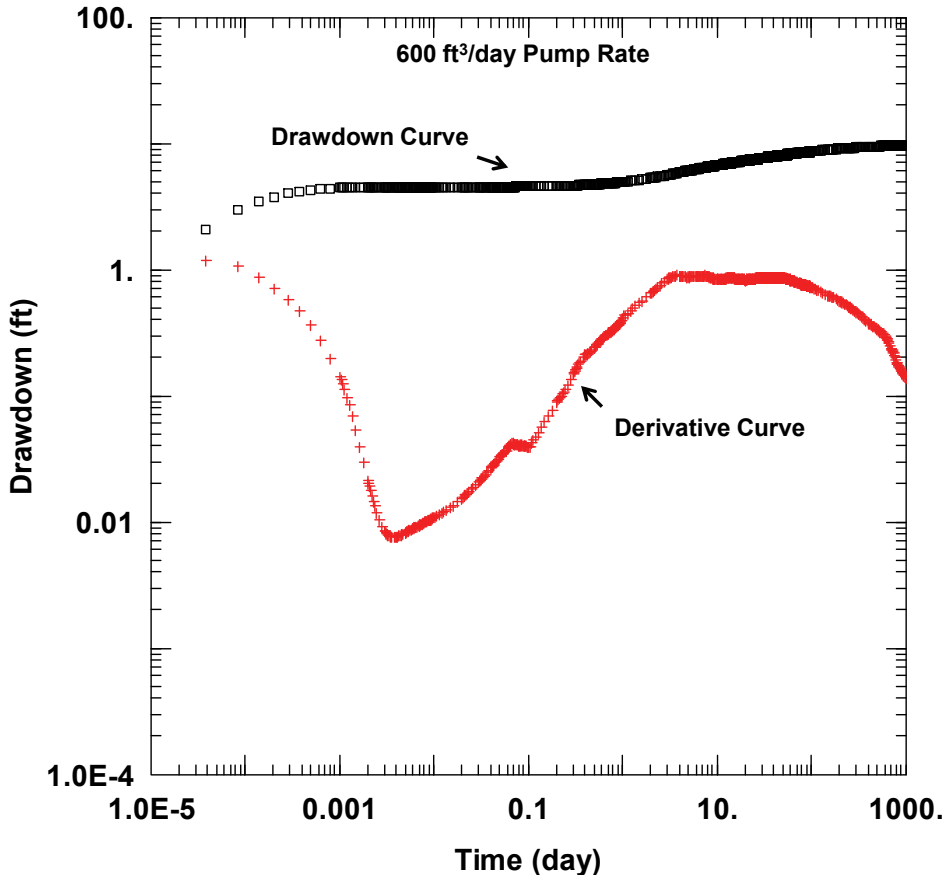

Figure 5-4. Log-Log plot of drawdown (black) and derivative (red) curves within the production well for the circular perched aquifer model. The production well was placed at the center of the perched aquifer and was pumped at a constant rate of 600 ft^3/day.

Changes in the slope of the derivative curve occurred at approximately 3, 40, and 600 days. Immediately following the "V" indicating the delayed-yield component of the intermediate time period, a near-horizontal derivative curve (approximately 3 days to 40

days) is observed. A horizontal derivative curve is often associated with the assumptions found in radial flow (Renard et al. 2009). Here, this segment reflects that the interactions of the sources, sinks, and boundaries were such that a modest decrease in the rate of drawdown occurred as the three dynamic water supplies (recharge capture, reduction in leakage, and storage) offset the demands of the well and remaining leakage. At 40 days, the derivative shows a sharp change to a negative slope. The negative slope reflects a decreasing rate of drawdown in the well as less water was lost through leakage and sustaining a larger aquifer, and was thus available to supply the well. A slight negative shift at 600 days reflects the additional decrease in the rate of drawdown as the total leakage rate approached the total extraction rate and the system moved toward equilibrium. The reduction in total leakage was 6% and 92% of the pump extraction rate at the 40 and 600 day inflection points, respectively.

We anticipated observing increased drawdown at late time due to encountering the perched-aquifer boundary. This would produce an increase in the slope of the drawdown and derivative curves. Changes in head at the periphery of the aquifer were observed to begin after approximately 20 days following the onset of pumping. This should correspond to the time that boundary effects would be fully engaged. However, an increase in drawdown was not observed and we conclude that boundary effects are overwhelmed by recharge and changes in leakage.

Given the dynamic model, it is acknowledged that other factors exist that can produce changes in drawdown along the periphery. Losses due to leakage decrease the aquifer thickness. A reduction in the maximum height of the aquifer decreases the radial gradient to the edge further reducing the aquifer flank thickness by lowering the angle of

the slope. Countering these factors is the tendency for outward lateral flow due to specified recharge conditions.

Simulations using pumping rates of 50, 100, and 1000 ft^3/day (representing 2%, 4%, and 40% of total recharge) showed similar patterns in the drawdown and derivative plots to those of the 600 ft^3/day pumping-rate test seen in Figure 5-4 (Figure 5-5). Using a lower pump rate produced only nominal change in the aquifer size, while the higher 1000 ft^3/day rate generates a noticeable reduction in height (8 ft) and footprint (60 ft). All tests exhibit a similar pattern of reduction in aquifer height and increased well drawdown dominant in the early stages of the test followed by a pronounced reduction in total leakage, analogous to the 600 ft^3/day pump rate test. At the completion of the simulation, the total reduction in leakage approached the respective pump rates for each test.

The drawdown and derivative curves for all well pumping rates also showed a decrease in the rate of drawdown at late time, easily viewed as the derivative curve shifts to a negative slope (Figure 5-5). The inflection point from positive to negative slope developed earlier in the lower pump rates as less reduction in leakage volume was required to offset the extraction rate. The ratios of the reduction of the total leakage rate to extraction rate at the inflection points are 8% for the 50 ft^3/day and 4% for the 100 ft^3/day pump rates, comparable percentages to that observed in the 600 ft^3/day pump rate. In both tests, drawdown was observed at the aquifer periphery at approximately 20 days, near the occurrence of inflection points on the derivative curve. However, as boundaries would be expected to produce an increase in the derivative slope rather than the prominent negative slope seen in the curves, the coincidence of the inflection point with a fully engaged boundary is not related.

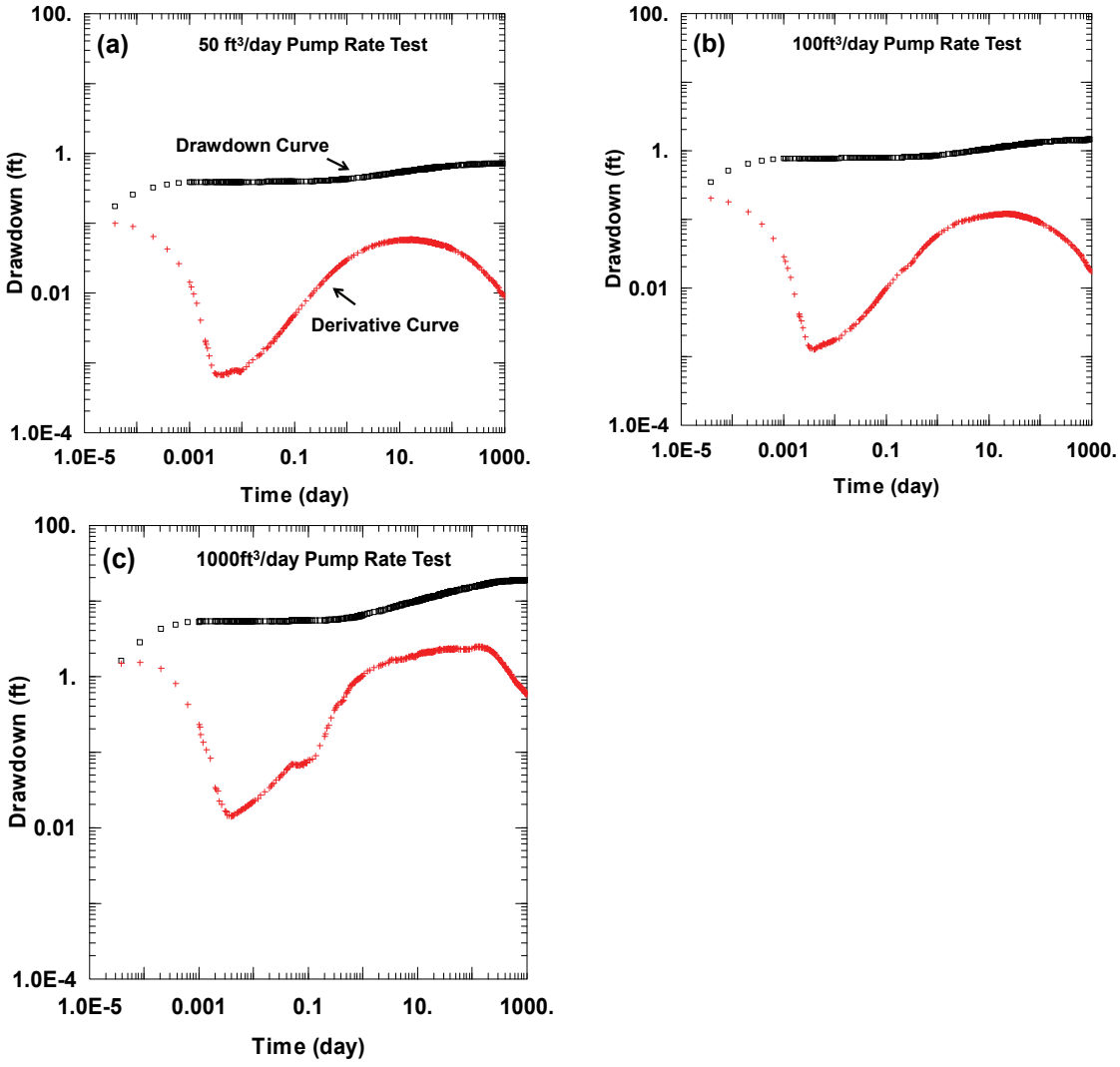

Figure 5-5. Log-Log plot of drawdown (black) and derivative (red) curves within the production well for the circular perched aquifer model for pumping rates of (a) 50, (b) 100, and (c) 1000 ft^3/day. The production well was placed at the center of the perched aquifer.

The overall response of the drawdown and derivative curves seen in the 1000 ft^3/day pump rate test was analogous to previous examples, yet some differences were

observed. The first is the increase in fluctuations in the derivative curve. These were likely numerical in origin, however they create uncertainties in identifying the inflection point to a negative slope derivative curve. A second distinction from the previous tests is the 0.2 positive slope of the derivative curve following the delayed-yield response. Two differing physical mechanisms may contribute to this pattern. As the pump rate has increased to 40% of the recharge rate, the extraction rate may be sufficiently large that boundary effects were no longer obscured by recharge. Techniques utilized in curve analysis describe flow regimes that depict positive slope-derivative curves, supporting the assertion that the increasing derivative curve observed in this simulation results from boundary effects (Cinco-Ley et al. 1981, Barker 1988). A second mechanism for the positive slope-derivative curve was a reduction in transmissivity as the increase in pumping rate created a thinner aquifer. This would increase the drawdown in the well. A high rate produces a deepening of the cone of depression and effective reduction of transmissivity at the wellbore (Hall 1996). Simple models were generated to assess the effects of pumping on a thin aquifer (Appendix B). Results from simulations of an infinite-in-extent unconfined aquifer of equivalent aquifer parameters produces a radial flow drawdown and derivative curve at low pump rates and a 0.15 positive slope-derivative curve at higher rates.

Off-Center Well Simulations

Placing the production well approximately 50 feet outside of the edge of the recharge area produced similar results to those described above. All other conditions remained the same. The observed physical processes suggest comparable behavior to the center well location. The aquifer thickness was approximately 12 feet at the well. Due to

the reduced transmissivity as compared to the center well location, simulations were conducted at lower pump rates of 100 and 300 ft^3/day which represent 4 and 12% of the total daily recharge rate, respectively. Figure 5-6 presents drawdown patterns through the center of the circular aquifer using a pumping rate of 300 ft^3/day after 1,000 days of pumping.

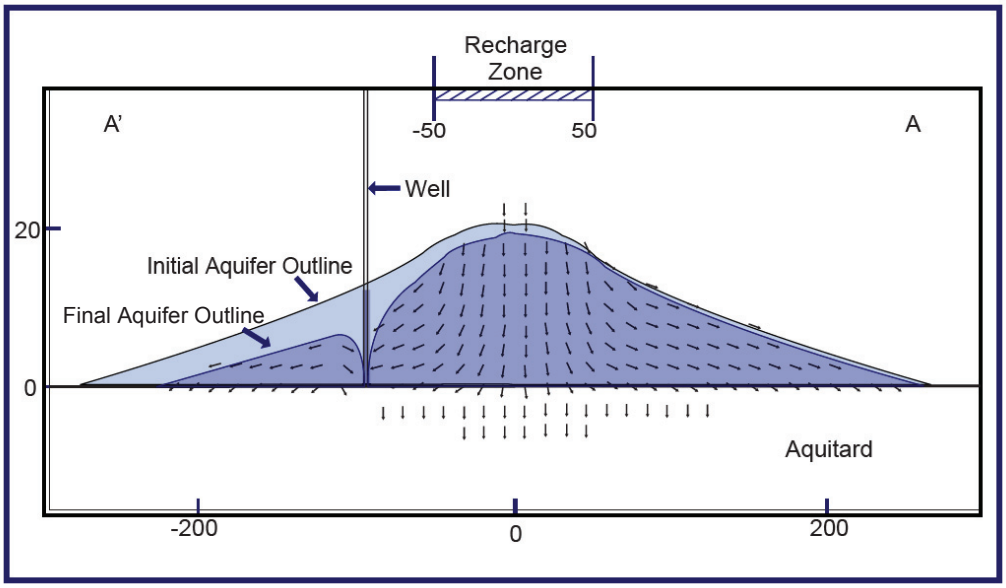

Figure 5-6. Cross section through the center of the circular perched aquifer after 1,000 days of pumping at 300 ft^3/day. The well is located 50 feet outside the recharge area. Outline in background shows the initial shape of the aquifer.

The flow path arrows indicate that recharge was captured along the flanks of the aquifer, eventually diminishing the supply of water to the down-gradient lobe. Initially, there was a decrease in aquifer thickness followed by a footprint reduction as leakage and pumping continually removed water from the system. A modest reduction in maximum aquifer height at the center of the aquifer is observed to be 0.2 ft in the 100 ft^3/ day test

and 0.7 ft for the 300 ft^3/day pump rate test. The time-drawdown and derivative behaviors were similar to those seen in the center well locations (Figure 5-7). During the early time period, the maximum height of the aquifer in the region of the well decreased which was mirrored in the well drawdown. The reduction in total leakage rate began at early time, increased throughout the test and approached the extraction rate at test completion. The off-center well locations also showed footprint reduction.

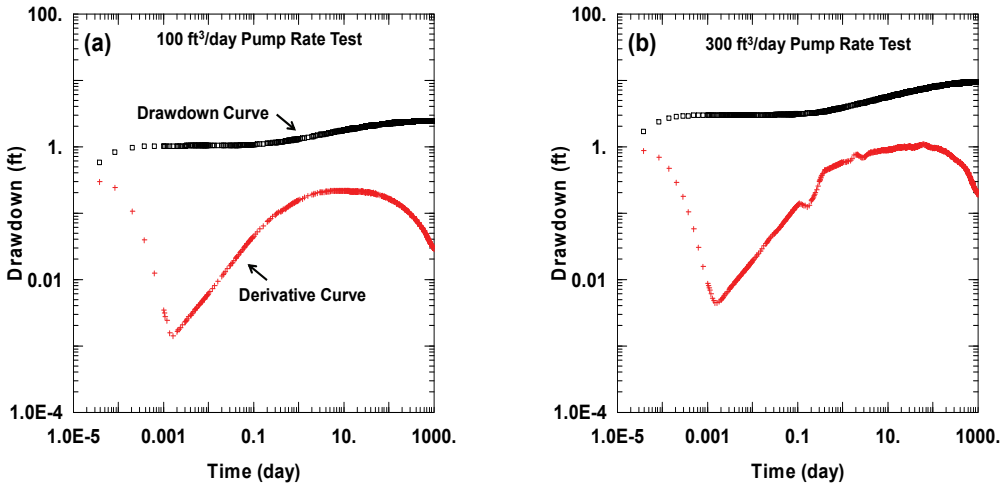

Figure 5-7. Log-Log plot of drawdown (black) and derivative (red) curves within the production well for the circular perched aquifer model for pumping rates of (a) 100 and (b) 300 ft^3/day. The production well was placed at 50 feet away from the edge of the recharge area.

The delayed-yield response was followed by the combined influences of pump extraction, increased capture of recharge, and initial reduction of leakage producing a near-horizontal curve at the lower pump rate and a positive slope at the 300 ft^3/day pump test. Derivative curves then increased in negative slope which coincided with footprint reduction and increased reduction of total leakage rate. In the 100 ft^3/day pump test, the

reduction in total leakage rate was 7% of the extraction rate at 40 days. The fluctuations in the 300 ft^3/day pump rate test create uncertainties in identifying the inflection point for the derivative curve. This point was approximately 60 days, corresponding to reduction in total leakage rates of 16% of the extraction rate. Observation points along the aquifer periphery near the pumping well (not shown) indicated initial drawdown at 8 days, and, near the periphery on the opposite side of the extraction well at 26 days. Surprisingly, late time boundary effects were still not prominently observed despite the closer proximity of the boundary. However, the response of the positive slope derivative in the 300 ft^3/day off-center pump test presents issues analogous to those discussed in the 1000 ft^3/day center well pump test (i.e. decrease in saturated thickness proximal to the wellbore and boundary influence no longer masked by recharge).

Edge Well Simulation

Simulations were also run placing the production well approximately 200 feet from the center of the aquifer and 80 feet from the aquifer edge. The aquifer was 4.5 ft thick at this location. Due to the decrease in transmissivity, the pump rate was reduced and simulations were run on 10 and 40 ft^3/day rates. To improve simulation results, the grid spacing adjacent to the well was reduced from 5 ft to 2.5 ft. The cross section of the 40 ft^3/ day pump test at test completion is shown in Figure (5-8).

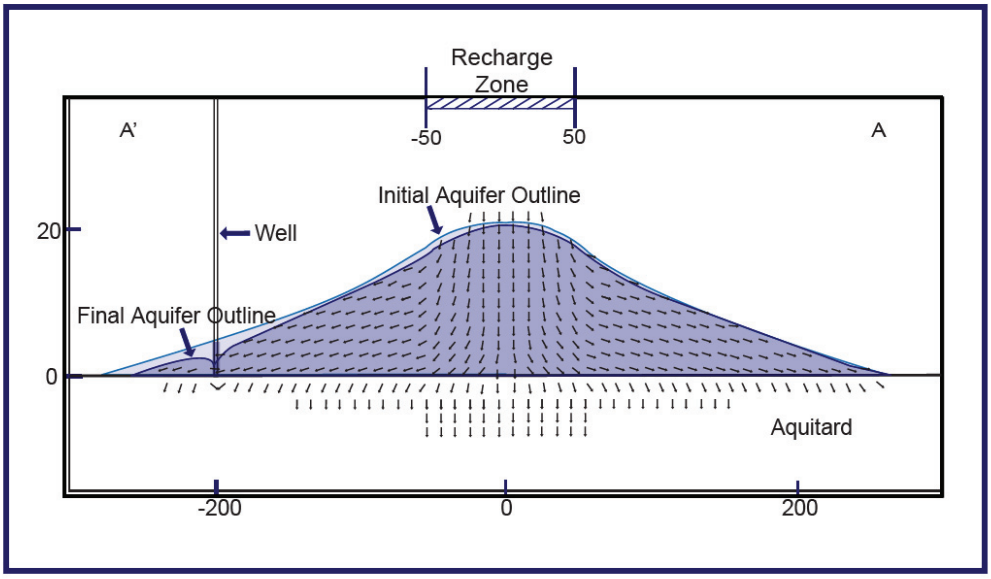

Figure 5-8. Cross section through the center of the aquifer after 1,000 days of pumping at 40 ft^3/day. The well is located 150 feet outside of the recharge area. Outline in background shows the initial shape of the aquifer.

Analogous to previous tests, simulations for both pump rates at the edge well location showed comparable interactions and resulting drawdown and derivative patterns (Figure 5-9). Again, the low pump rate produced a near-horizontal derivative curve while the higher pump rate of 40 ft^3/day resulted in a positive slope-derivative curve at late time. Both simulations exhibit inflection points on the derivative curve once total leakage rates were reduced. The 10 ft^3/day pumping rate test showed an inflection point after the reduction of the total leakage rate equaled 6% of the extraction rate. The 40 ft^3/day pumping rate test exhibited an inflection point once the reduction in the total leakage rate was 25% of the extraction rate. Observation points at the periphery of the aquifer near the edge well suggests the boundary was encountered at approximately 4.5 days and along

the edge on the opposite side of the pumping well at 45 days. However, the boundary impact on the drawdown curve was indistinguishable from influences of recharge, leakage, and pumping, except as previously noted in the higher pumping-rate tests.

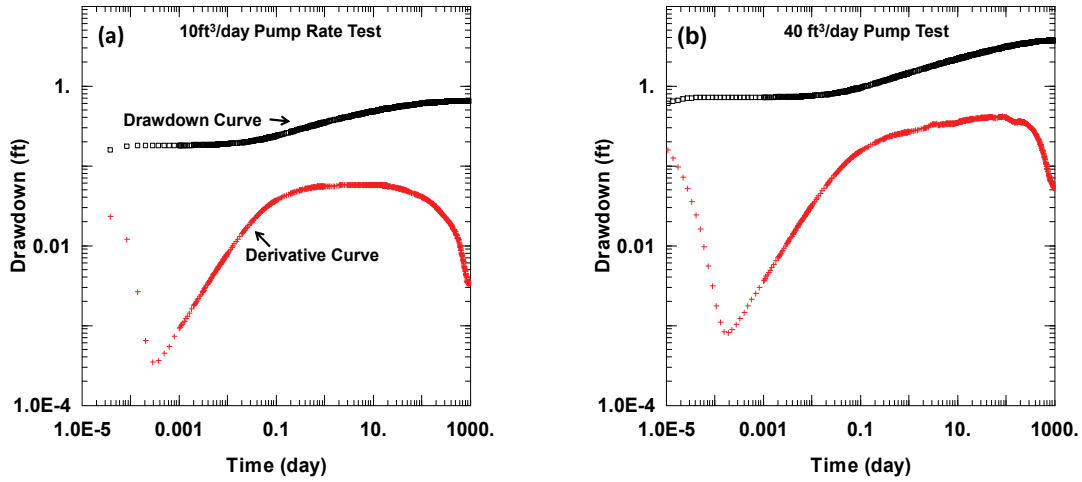

Figure 5-9. Log-Log plot of drawdown (black) and derivative (red) curves within the production well for the circular perched aquifer model for pumping rates of (a) 10 and (b) 40 ft^3/day. The production well was placed approximately 200 feet from the center of the aquifer.

Tight-Aquifer Simulations

The results for the circular aquifer model using the lower hydraulic conductivity of 0.2 ft/day exhibit similar relationships and patterns in the drawdown and derivative curves to those observed in the higher hydraulic conductivity simulations. The sequence of processes was comparable to the higher 3.0 ft/day hydraulic conductivity test discussed above. However, in contrast to the 3.0 ft/day hydraulic conductivity models, the lower hydraulic conductivity tests showed a continued increase in the total leakage

rate throughout the test indicating that the system never approached steady-state conditions between pumping, leakage, and recharge (Figure 5-10). Leakage was markedly less than total extraction rate after 10,000 days. Hydraulic resistance (ratio of the thickness of the aquitard, b', to the hydraulic conductivity of the aquitard, K') serves as an example of the impact in aquifer response due to the different hydraulic conductivities. The hydraulic resistance is 1,000,000 days in the 0.2 ft/day hydraulic conductivity model and 6,667 days in the 3.0 ft/day hydraulic conductivity model which reflects a factor of 150 in the ability to transmit water through the aquitard. Figure 5-10 provides an example of the results found in the low hydraulic conductivity simulations. Figure 5-11 depicts the drawdown and derivative curve. These figures convey the same processes but the increased duration of the test required to produce an analogous response to the higher hydraulic conductivity is greater than an order of magnitude.

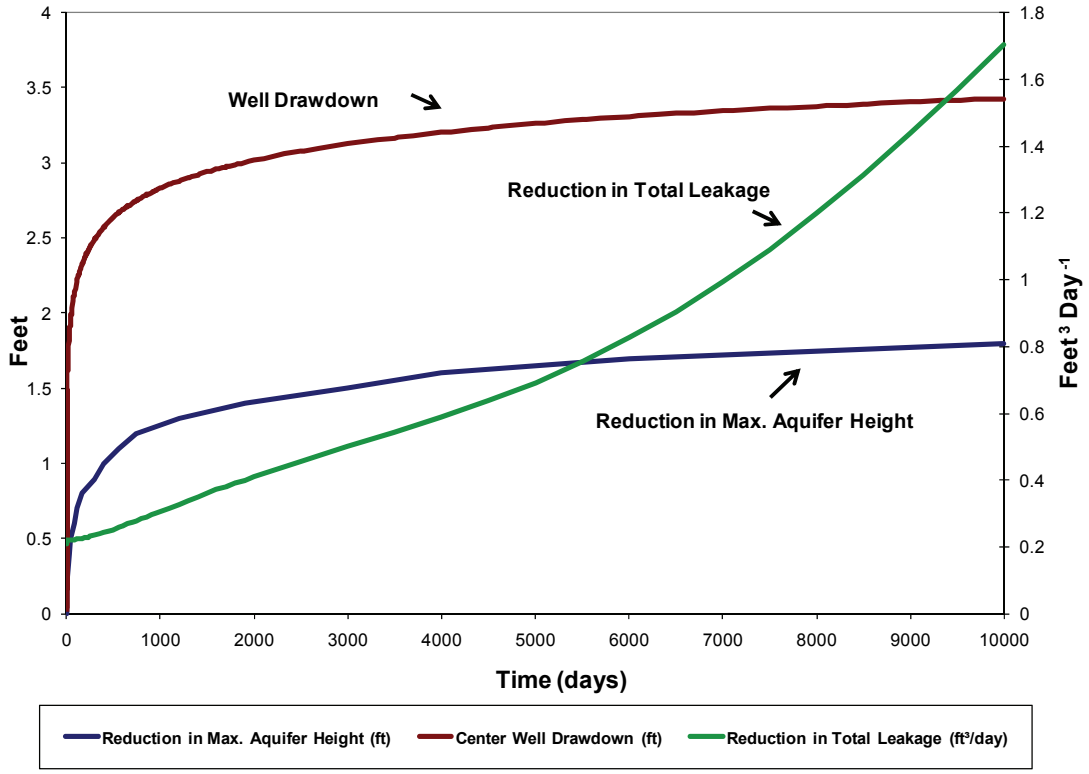

Figure 5-10. Changes in drawdown (brown line), total leakage (green line), and aquifer height (blue line) for the circular perched aquifer with low hydraulic conductivity. The production well was located at the center of the perched aquifer and pumped at a constant rate of 10 ft^3/day.

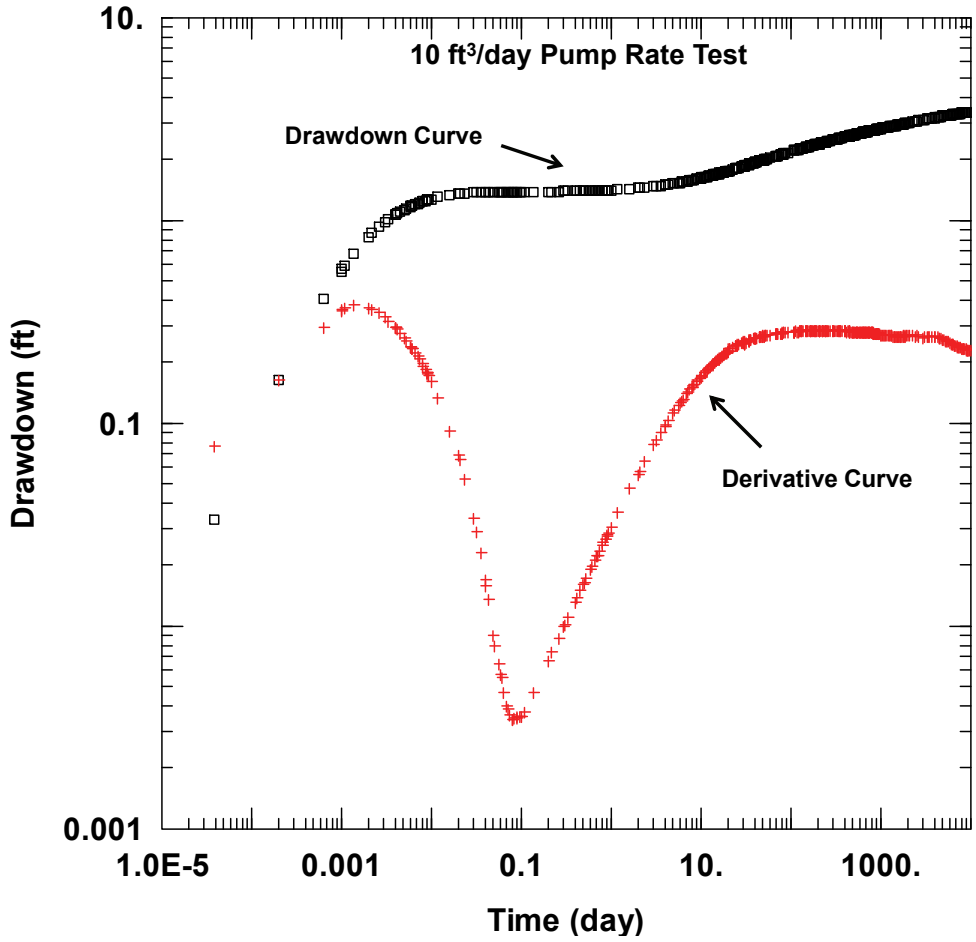

Figure 5-11. Log-Log plot of drawdown (black) and derivative (red) curves within the production well for the circular, 0.2 ft/day hydraulic conductivity, perched aquifer model at 10 ft^3/day pumping rate. The production well was in the center of the aquifer.

Rectangular Model

The rectangular models were initialized in a comparable manner to the circular models. The simulations started with a hydrostatic zero head on which a constant-rate linear recharge was imposed to develop the rectangular perched aquifer. Simulations using the 3.0 ft/day hydraulic conductivity aquifer reached quasi steady-state after 11

years. The lower hydraulic conductivity (K = 0.2 ft/day) perched aquifer models required approximately 550 years to stabilize. These quasi steady-state heads were imported into identical models and constant rate pumping tests were conducted in two differing well locations within the perched aquifer. The model length was sufficient that the distal boundaries of the model were not encountered by the radius of influence of the production well. Table 4-1 and 4-2 provides the pumping rates and aquifer parameters.

Results for the rectangular models were comparable to the respective circular models in the both the 3.0 ft/day and 0.2 ft/day hydraulic conductivity simulations. The tight aquifer (K = 0.2 ft/day) required lower pumping rates to prevent dewatering and a lengthy test duration (10,000 days) to produce comparable curve patterns to those observed in the higher hydraulic conductivity simulations. Figure 5-12 shows the drawdown and derivative curves for 3.0 ft/day hydraulic conductivity model for the center and edge pumping locations. As the dominant physical processes were the same, the drawdown response was analogous to the circular models. Again, a negative slope-derivative curve developed as leakage in the region of the well was lessened by a reduction in aquifer height and/or footprint. At higher rates or as the well was positioned at the edge of the aquifer, a positive slope-derivative curve was again noted. Results showed a positive slope-derivative curve of 0.5 to 0.6. Based on the results, the mechanisms for the positive slope seen in the rectangular perched aquifer simulations were as for those described for the circular perched aquifers. That is, the effects of reduced transmissivity and increased boundary impact, produced indistinguishable influences on the drawdown curve response.

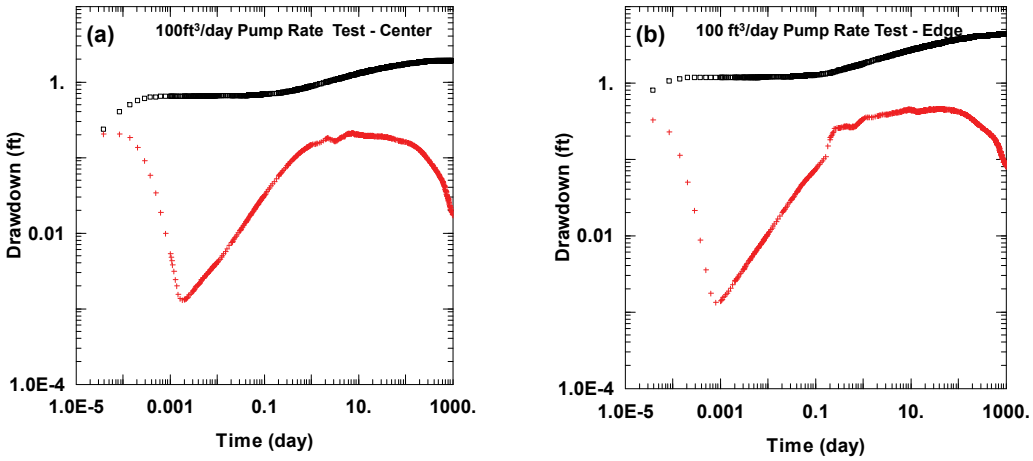

Figure 5-12. Rectangular model center and edge well locations drawdown and derivative curves for 100 ft^3/day pump rate tests using an aquifer hydraulic conductivity of 3.0 ft/day.

Transmissivity Estimates

As discussed above, the response of a perched aquifer to pumping produces a complex time-drawdown. Nevertheless, the leaky perched aquifer simulations provided an opportunity to evaluate a method to estimate transmissivity values. Below, we used simulated time-drawdown data to develop a simplified methodology to measure aquifer parameters yet may be applicable to field operations.

The preceding sections of this chapter have shown that the thickness of the leaky perched aquifer changed as a result of spatial and temporal variations in head rendering transmissivity a dynamic value. Therefore, seeking a single representative transmissivity parameter for the perched system is of limited use. Analysis of the drawdown curves used in this study suggests that the hydraulic conductivity is a more suitable parameter to obtain from the drawdown curves. Knowing the estimated hydraulic conductivity allows

for re-calculation of transmissivity values due to changes in aquifer thickness. Storage values were also examined but did not provide useful results.

To assess hydraulic conductivity, the Cooper-Jacob straight-line method (Cooper and Jacob 1946) with drawdown correction for unconfined aquifers (Jacobs 1944) was found to produce consistent results. Figure 5-13 depicts the process to determine the hydraulic conductivity. The figure presents semilog plots of the drawdown and derivative curves for simulations conducted with the sand texture and center well location for two pumping rates (50 ft^3/day and 600 ft^3/day). First, the time at which the delayed-yield interval ends was located on the derivative curve; then the corresponding point on the drawdown curve was found. The tangent line to this point was then estimated. The results of the 50 ft^3/day pumping-rate test showed that the gentle slope of the derivative curve created difficultly in identifying the completion of delayed-yield response and thus the point at which the straight line should be fit to the drawdown curve. As drawdown during the pump test was low, fitting the curve further away from the end of the delayed-yield response did not significantly affect the results. The 600 ft^3/day pumping-rate test had an easily identified point for the completion of the delayed yield. This point was then used to establish the tangent line to the drawdown curve. Due to the physical processes previously described in this study, the reducing slope of the drawdown curve near the completion of the simulation deviated from the straight line.

The transmissivity value was determined for this tangent line in accordance with the Cooper-Jacob straight-line method. By assuming that the loss of aquifer height was negligible immediately following the delayed-yield component, the transmissivity value was divided by the initial thickness of the perched aquifer to obtain hydraulic

conductivity (in field operations, the initial thickness of the perched aquifer would be ascertained from drilling operations). To estimate transmissivity values at differing locations within the perched aquifer or as a result of decreasing aquifer height from pumping, the hydraulic conductivity value can be multiplied by various aquifer thicknesses.

Using this technique, hydraulic conductivity for simulations in this study were estimated. Table 5-1 and Figure 5-14 present the results. As shown, the hydraulic conductivities were comparable to the simulation input values of 3.0 ft/day and 0.2 ft/day for the fine sand and silt textures respectively. All results were slightly higher than the input parameter, most notably in the higher pumping-rate simulations.

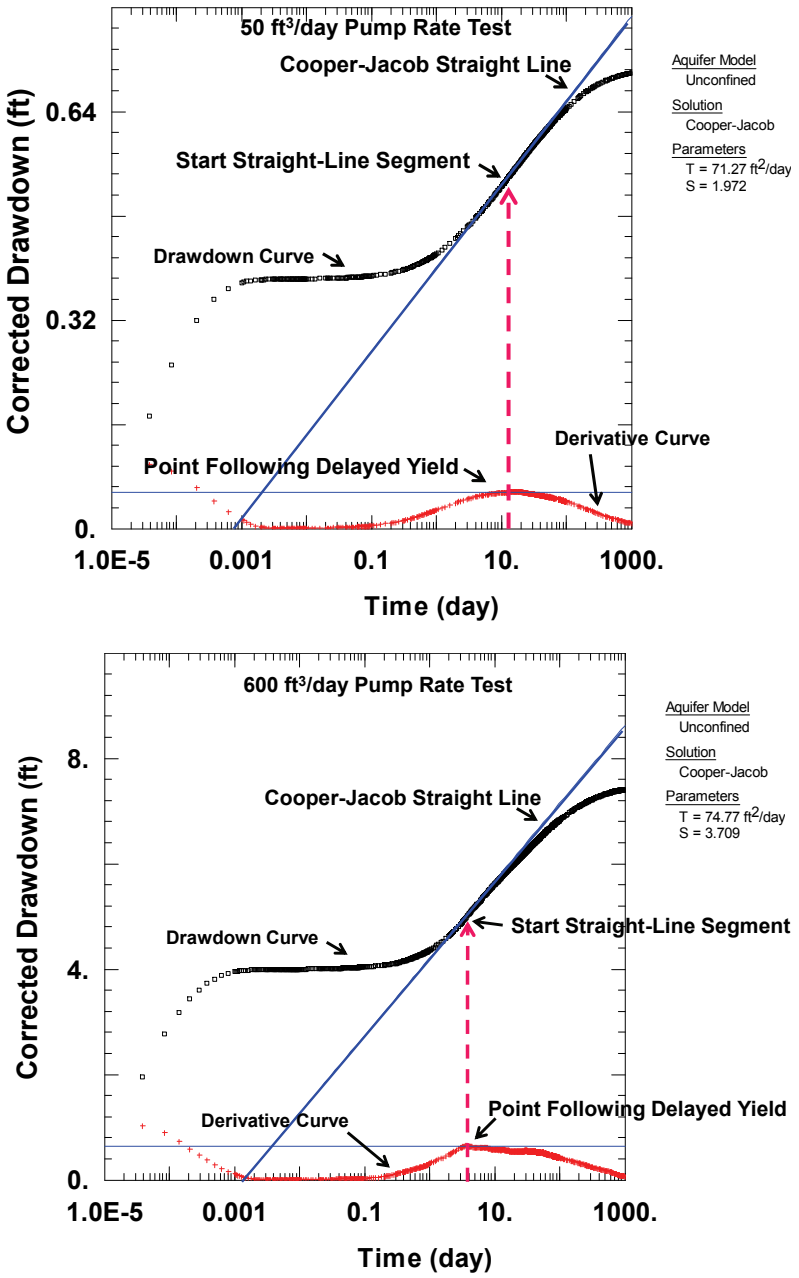

Figure 5-13. Examples of estimating the initial transmissivity value using the Cooper-Jacob straight-line method. The semilog plots depict drawdown (black) and derivative (red) curves from the circular aquifer, K = 3.0 ft/day, center well locations. Upper plot is 50 ft^3/day pumping rate and lower is 600 ft^3/day pumping rate.

Shape	Tex	Well Loc.	Pump Rate (ft^3/day)	Start Time of Straight line	K (ft/day)	b (ft)	Predict. T (ft^2/day)	Simul. T (ft^2/day)	Simul. K (ft/day)
C	S	Cent	50	13 days	3.0	21	63	71	3.4
			100	14 days	3.0	21	63	73	3.5
			600	3 days	3.0	21	63	75	3.6
			1000	2.6 days	3.0	21	63	80	3.9
		Off-Cent	50	7 days	3.0	12	36	38	3.1
			100	3.6 days	3.0	12	36	41	3.3
			300	4 days	3.0	12	36	44	3.6
		Edge	10	0.6 days	3.0	4.7	14	16	3.3
			40	0.5 days	3.0	4.7	14	17	3.7
	Silt	Cent	10	40 days	0.2	14	2.8	3.6	0.25
			25	22 days	0.2	14	2.8	4.2	0.29
		Off-Cent	10	30 days	0.2	10	2.0	2.3	0.22
		Edge	2	25 days	0.2	5.3	1.1	1.1	0.22
R	S	Cent	100	1.2 days	3.0	14	42	50	3.7
			300	1 day	3.0	14	42	48	3.5
		Edge	100	1 day	0.2	8.0	1.6	28	3.5
	Silt	Cent	2	25 days	0.2	12	2.4	2.6	0.22
		Edge	2	30 days	0.2	6.1	1.2	1.3	0.22

Table 5-1. Computed and predicted transmissivity and hydraulic conductivity values for simulations in this study. Abbreviations: C is circular; R is rectangular; Tex is texture; S is sand; Loc. is Location; Cent is center; Predict is predicted; T is transmissivity; b is aquifer thickness; K is hydraulic conductivity; Simul is simulation.

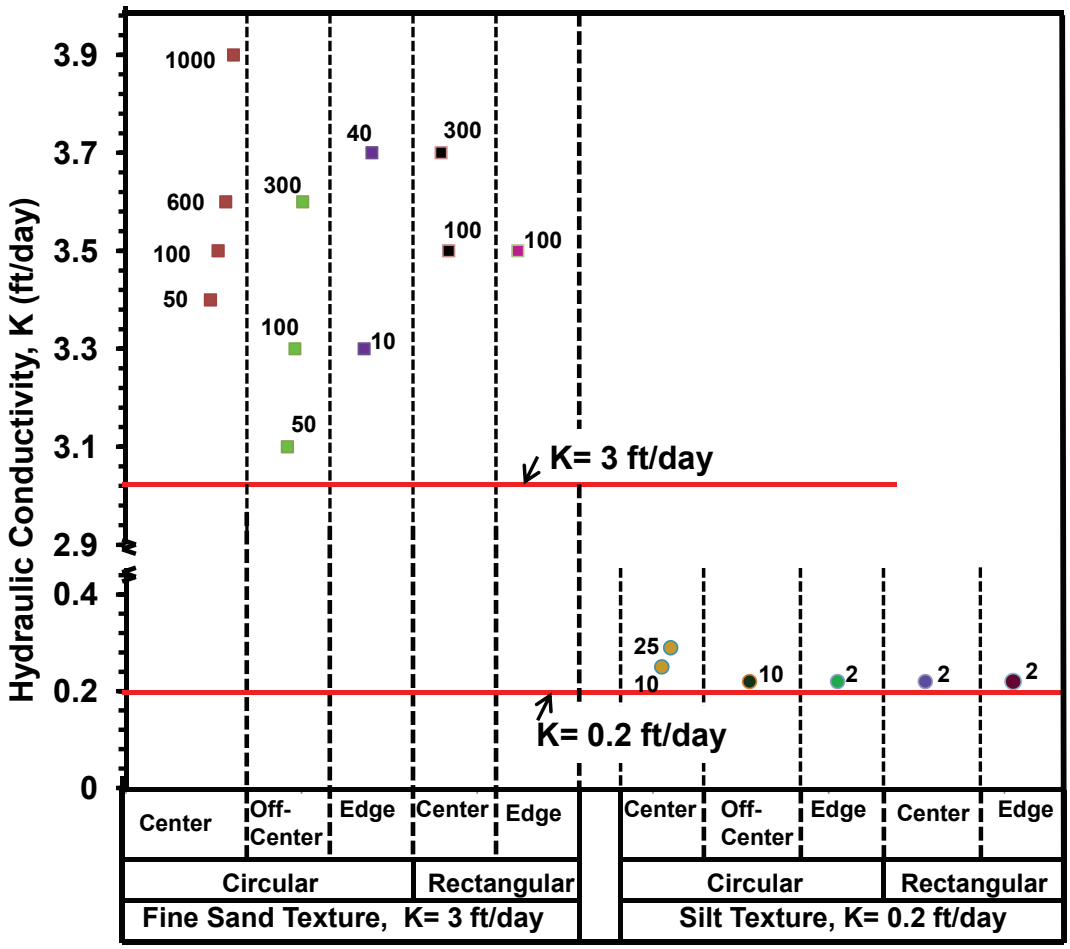

Figure 5-14. Estimated hydraulic conductivity values for simulations presented in this study using the Cooper-Jacob straight-line method tangent to the drawdown curve immediately following the delayed-yield response. Values adjacent to the data point represent the simulation pumping rate in ft^3/day. The squares and circles represent the high (3.0 ft/day) and low (0.2 ft/day) hydraulic conductivity model runs, respectively.

Applicability of Time Constraints to Field Investigations

Results from this study have shown that the drawdown curves from constant-rate pump tests can assist in differentiating a leaky perched aquifer from an infinite in areal extent aquifer by the appearance of a negative slope-derivative curve. Furthermore,

simulation results suggest that the drawdown and derivative curves provide a reliable hydraulic conductivity to permit the calculation of the varying transmissivity. For these findings to be of value to field investigations, the data must be obtained within practical time constraints.

Although the silt model (hydraulic conductivity of 0.2 ft/day) required excessive test durations (~2,000 days), the fine sand model (hydraulic conductivity of 3.0 ft/day) produced informative results within reasonable time intervals (~20 days). Simulations demonstrated that the appearance of the negative slope-derivative curve suggesting a leaky perched aquifer formed earlier at low pumping rates as the aquifer did not require a large reduction in size to approach a new equilibrium. Therefore, by use of low extraction rates, the first appearance of the negative slope on the derivative curve was achieved within plausible time periods for field tests. Figure 5-5 shows an example of the onset of the inflection point and differing pumping rates. In the 50 ft^3/day pumping-rate test, the inflection point is located at approximately 20 days, an order of magnitude less than that of the 1,000 ft^3/day pumping-rate test.

The response of the aquifer to constant pumping is observed sooner in higher hydraulic conductivity formations. When the models presented in this investigation were scaled to higher hydraulic conductivities, comparable leaky perched aquifers were generated. Figure 5-15 shows an example where the hydraulic conductivity of the perched aquifer was increased from 3.0 ft/day to 300 ft/day with other model parameters scaled accordingly. The drawdown and derivative curves show analogous patterns to the hydraulic conductivity of 3.0 ft/day but developing over a shorter duration.

Therefore, the 3.0 ft/day hydraulic conductivity tested in this study yielded a negative slope-derivative curve in a reasonable time period if the low pumping rates were used. However, these results may represent the lower range of transmissivities capable of producing meaningful results within acceptable time constraints for field applications. Higher hydraulic conductivity formations required less time to obtain useful data due to the faster response of the formation.

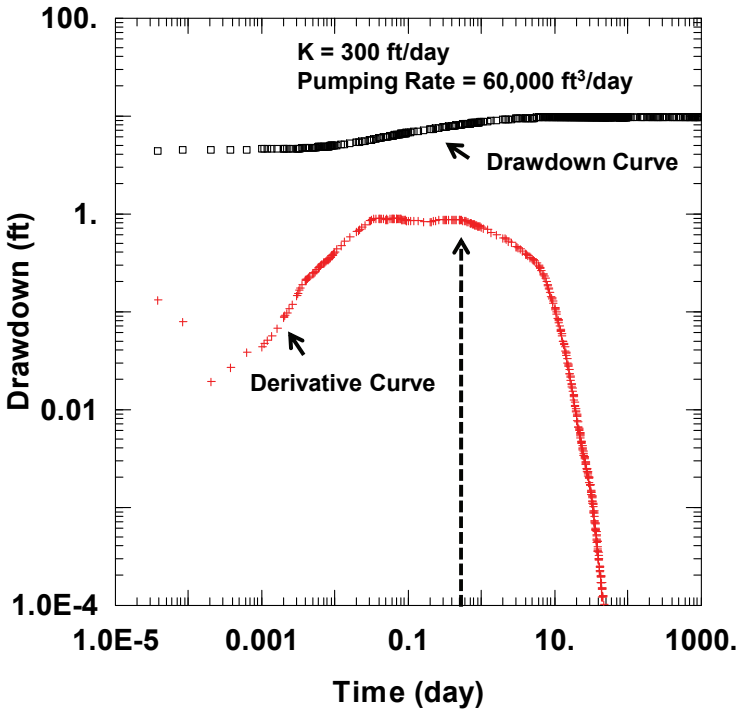

Figure 5-15. Log-Log drawdown and derivative curve for the constant-rate pump test conducted in a simulated perched aquifer of hydraulic conductivity 300 ft/day resulting in a shorter duration for the completion of the delayed-yield response and development of the negative slope-derivative curve.

As discussed in the preceding section, using the Cooper-Jacob straight-line method provided reasonable estimates of hydraulic conductivity that could then be used

to assess the variable transmissivity. As the point from which the straight line was determined was obtained immediately following the delayed-yield response, all time periods for models using the hydraulic conductivity of 3.0 ft/day were practical for field applications. The hydraulic conductivity values were closest to the predicted parameter at lower pump rates, further supporting the use of reduced pumping rates in field operations.

CHAPTER 6 - CONCLUSIONS

The purpose of this study was to ascertain if particular and unique responses of a constant-rate pump test in a leaky perched aquifer receiving recharge can identify the aquifer: 1) as limited in lateral extent, 2) of a particular geometry, and 3) the well position within the perched aquifer. Simulation results showed a consistent late-time response that identified the limited size of the perched aquifer. Specifically, the simulations showed extraction demands were initially met by recharge and storage. As less recharge was available to sustain the aquifer due to pumping and continued leakage through the aquitard, the size of the aquifer diminished by a decrease in lateral footprint and/or thickness. The reduced size of the aquifer and reduced head lessened the total volume leaked through the aquitard, which provided more recharge water to meet the demands, reducing the rate of drawdown in the well as the system approached a new steady-state. The decrease in rate of drawdown is expressed as a negative slope on the derivative curve. Figure 6-1 depicts the generalized contribution of sources delivered to the well and corresponding response of the drawdown curve. The well supply at early time (A) was met from wellbore and elastic storage. Following this period, a delayed-yield response was observed indicating the dominance of water delivered to the well from specific yield (B), after which the expanding cone of depression provided a greater component by increased interception of recharge entering the perched aquifer. Over time, the expanding

cone of depression and capture of recharge delivered the bulk of water to the well (C), and, as the aquifer size was further reduced, the system approached equilibrium (D).

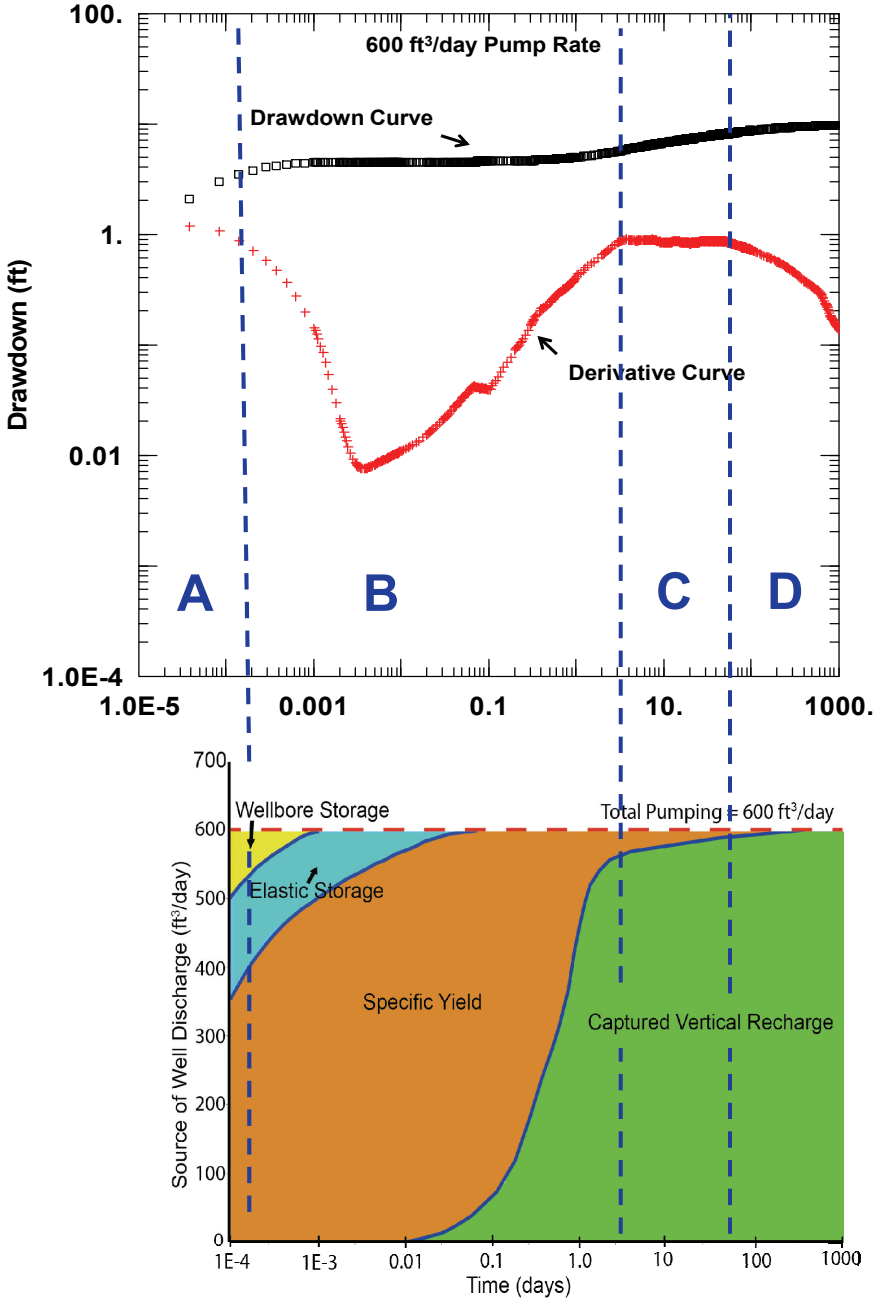

Figure 6-1. Schematic of water sources to the well and corresponding drawdown and derivative curve. The lag time of the delayed-yield component is not incorporated in the water source graph. Segments A, B, C, and D represent major shifts in the well supply and drawdown curve.

It is the constrained size of the leaky perched aquifer with constant recharge that allows for the development of a new equilibrium by reduction of the aquifer size. As the system approaches a new steady-state, a decrease in the rate of drawdown is observed in the extraction well. This repeatable pattern of a late time negative slope-derivative curve is in contrast to the infinite-in-extent unconfined aquifer seen in Figure 1-2(a) where the derivative curve shows a late time horizontal line identifying radial flow associated with infinite-in-extent aquifers.

Thus, the first objective of the study is met as the observation of the negative slope-derivative curve can assist in differentiating a leaky perched aquifer receiving recharge from an infinite-in-extent unconfined aquifer. However, the remaining goals of ascertaining the geometry and position of the well within the perched aquifer were not achieved as the simulations indicate that boundary effects and aquifer geometry are masked by other late-time processes.

As depicted in all the simulations, the overriding mechanism at late time is the increased capture of recharge, reduction of aquifer size, and decrease in total leakage providing an increase in water supply to the well. It is the response of the drawdown curve to this mechanism that dominates the behavior of the curve. The system is dynamic and the changing impact of recharge, leakage, pumping, and boundaries combine to create the appearance of the drawdown and derivative curves.

Data obtained from this study presented an opportunity to examine a method for estimating transmissivity. An evaluation of the simulated drawdown curves using the Cooper-Jacob straight-line method was conducted on the tangent to the point

immediately following the delayed-yield effect. Aquifer test-analysis using this straight-line slope produced comparable hydraulic conductivity values to the model input parameters. Determining the hydraulic conductivity allows transmissivity values to be calculated according to the spatial and temporal changes of aquifer thickness in the leaky perched aquifer.

As the simulations were conducted using low pumping rates with small drawdowns over lengthy test durations, the results of this study were reviewed for feasibility to field investigations. Assessments showed the small drawdown in the pumping well can be measured using appropriate field equipment and by use of low pumping rates the duration to obtain meaningful data is achieved within practical time periods for field operations. The lower pumping rates required less reduction in aquifer size for the system to return to equilibrium, therefore, the appearance of the negative slope-derivative curve developed sooner than for simulations at higher pumping rates. Additional considerations supporting the use of a low pumping rate for fieldwork were the improved hydraulic conductivity estimates as compared to those obtained from higher pumping rates and the avoidance of a positive slope-derivative curve. Tests showed that a thin, infinite-in-extent aquifer could exhibit a positive slope-derivative curve at high pump rates. As a positive slope-derivative curve is often attributed to boundary influences, the use of a lower pump rate may avoid erroneous identification of aquifer boundaries when the system is actually an infinite-in-extent aquifer.

Components of this study may be extended to perched aquifers formed by differing hydrological environments. For example, a perched aquifer formed on a localized aquitard with recharge covering most of the perched zone would likely develop

comparable drawdown patterns. In this case, leakage would be replaced by groundwater movement over the periphery of the aquitard. However, given the diversity of features that may be involved in the development of a perched aquifer, additional numerical exploration to determine the resultant drawdown curves is merited. Although the systems described are highly nonlinear, investigation into the development analytical solutions focusing on leakage and pumping effects should be considered.

REFERENCES

Anakhaev, K.N. 2009. A particular analytical solution of a steady-state flow of a groundwater mound. Water Resources. 36 (5) pp.507-512.

Bagtzoglou, A.C. 2003. Perched water bodies in arid environments and their role as hydrologic constraints for recharge rate estimation: Part 1. A modeling methodology. Environ. Forensics v. 4(1), p. 39-46.

Barker, J.A. 1988. A generalized radial-flow model for pumping tests in fractured rock. Water Resources Research. 24, 1796-1804.

Behera, S., Jha, M.K., Kar, S. 2003. Dynamics of water flow and fertilizer solute leaching in lateritic soils of Kharagpur region, India. Agricultural Water Management. 63(2), p.77-98.

Boulton, N.S. 1954. The drawdown of the water-table under non-steady conditions near a pumped well in an unconfined formation. Proceedings of the Institution of Civil Engineers, London, great Britain, Part III, p.564-579.

Bourdet, D., Ayoub, J.A., Pirard, Y. M. 1989. Use of pressure derivative in well-test interpretation. Society of Petroleum Engineers Formation Evaluation. June. 293-302.

Bouwer, H., Back, J., Oliver, J.M. 1999. Predicting infiltration and ground-water mounds for artificial recharge. Journal of Hydrological Engineering. 4 (4), pp. 350-357.

Cinco-Ley, H., Samaniego-V. F. 1981. Transient pressure analysis for fractured wells. Journal of Petroleum Technology. September. 1749-1766.

Cooper, H.H., Jacob, C.E. 1946. A generalized graphical method for evaluating formation constants and summarizing well field history, Transactions, American Geophysical Union. 27, p.526-534.

Cozzarelli, I.M., Herman, J.S., Baedecker, M.J. Fischer, J.M. 1999. Geochemical heterogeneity of a gasoline-contaminated aquifer. Journal of Contaminant Hydrology. 40 (3) , pp.261-284.

Driscoll, F.G. 1986. Groundwater and Wells, Second Edition. U.S. Filter/Johnson Screens, St. Paul, Minnesota. 1089 p.

Duffield, G.M. 2007. AQTESOLV for Windows Version 4.5. User's Guide, HydroSOLVE, Inc., Reston, Virginia.

Ferris, J.G., Knowles, D.B., Brown, R.H., Stallman, R.W. 1962. Theory of aquifer tests. U. S. Geological Survey Water-Supply Paper. 1536-E, 69-174.

Fetter, C.W. 1994. Applied Hydrogeology, third edition. Macmillan College Publishing Company, New York, N.Y. 691p.

Fogg, G.E., Fleckenstein, J., Niswonger, R.G., Rains, M.C., and Williamson, R.J. 2003. Perched aquifer hydrology: An Unexplored Frontier? Geological Society of America Abstracts with Programs, Vol. 35, No. 6, September 2003, p.449.

Hall, P. 1996. Water Well and Aquifer Test Analysis. Water Resources Publications, LLC, Highlands Ranch, Colorado. 412 p.

Hantush, M.S., Jacob, C.E. 1955. Non-steady radial flow in an infinite leaky aquifer. Transactions, American Geophysical Union. 36 (1), 95-100.

Hueni, C. 2010. Current Status Report: Pantex Plant (USDOE), EPA ID # TX4890110, Site ID 0604060, EPA region 6. url: http://www.epa.gov/region6/6sf/pdffiles/0604060.pdf. Accessed December 20. 2010.

HydroGeoLogic, Inc. 2007. MODFLOW-SURFACT Software (Version 3.0) Overview:

Installation, Registration and Running Procedures. Herndon, VA.<www.hgl.com>.

Jacob, C.E., 1944. Notes on determining permeability by pumping tests under water-table conditions. U.S. Geological Survey Mimeo Report, US Geological Survey, Reston, VA.

McDonald, M.G., Harbaugh, A.W., 1988. A modular, three-dimensional finite difference ground-water flow model: US Geological Survey Techniques of Water-Resources Investigations, book 6, chap.A1. 586 p.

Moench, A.F.1995. Combining the Neuman and Boulton models for flow to a well in an unconfined aquifer. Ground Water. 33(3), p. 378-384.

Neuman, S.P. 1972. Theory of flow in unconfined aquifers considering delayed response of the water table. Water Resources Research. 8 (4), 1031-1044.

Neuman, S.P. 1974. Effect of partial penetration on flow in unconfined aquifers considering delayed gravity response. Water Resources Research. 10 (2), 303-312.

Panday, S., Huyakorn, P.S. 2008. MODFLOW SURFACT: A state-of-the-art use of vadose zone flow and transport equations and numerical techniques for environmental evaluations. Vadose Zone Journal. 7 (2), 610-631.

Phillips, Owen M. 1991. Flow and Reactions in Permeable Rocks. Cambridge University Press, New York, NY. 285 p.

Rains, M.C., Fogg, G.E., Harter, T., Dahlgren, R. A., Williamson, R.J., 2006. The role of perched aquifers in hydrological connectivity and biogeochemical processes in vernal pool landscapes, Central Valley, California. Hydrological Processes. 20. 1157-1175.

Reichard, E.G., Izbicki, J.A., Martin, P. 1995. Implications of uncertainty in exposure assessment for groundwater contamination. Proceeding from the Rome Symposium, September 1994, Assessing and Managing Health Risks from Drinking Water Contamination: Approaches and Applications. IAHS Publ. no 235, pp. 211-219.

Renard, P., Glenz, D., Mejias, M. 2009. Understanding diagnostic plots for well-test interpretation. Hydrogeology Journal. 17, 589-600.

Schlumberger, 2009. Visual MODFLOW Software (Version 2009.1 Pro) Developed by Schlumberger Services.

Schwartz, F.W., Zhang, H. 2003. Fundamentals of Ground Water. John Wiley & Sons, New York, NY. 583 p.

Serrano, Sergio E. 2003. Modeling groundwater flow under transient nonlinear free surface. Journal of Hydrologic Engineering.8(3), p.123-132.

Theis, C.V. 1935. The relationship between lowering of the piezometric surface and the rate and duration of discharge of a well using groundwater storage. Transactions, American Geophysics Union. 16, 519-524.

Walker, D.D., Roberts, R.M. 2003. Flow dimensions corresponding to hydrogeologic conditions. Water Resources Research. 39 (12), 1349-1356.

Wu, Y.S., A.C. Ritcey, and G.S. Bodvarsson. 1999. A modeling study of perched water phenomena in the unsaturated zone at Yucca Mountain. Journal Contam. Hydrol. V. 38 (1-3), p. 157-184.

APPENDIX A - VERIFICATION OF MODELING SOFTWARE

The MODFLOW-SURFACT (HydroGeoLogic, Inc. 2007) simulations and Aqtesolv (Duffield 2007) drawdown and time-derivative curves were verified for the ability of the software to produce the predicted aquifer parameters and the anticipated response to boundaries when constant-rate pump tests were imposed. Two sets of simple rectangular models were constructed. The first group simulated aquifers of infinite areal extent to assess predicted versus computed parameter estimation. The second set of models assessed an aquifer of limited extent for appropriate drawdown and derivative curve behavior when the cone of depression uniformly encountered model no-flow boundaries.

Infinite-in-Extent Models

Analytical solutions and the graphical depictions, or type curves, are used to determine the transmissivity of an aquifer by comparing drawdown curves generated from constant-rate pump tests to the analytically derived type curves. The solutions assume infinite-in-extent aquifers. To verify the ability of the software to produce transmissivity values comparable to those calculated from the input parameters, this type-curve matching technique was performed on simulated data generated from models mimicking infinite-in-extent conditions. The dimensions for the infinite areal extent model were 20,000 ft in length (L) by 20,000 ft in width (W) by 10 ft in height (H).

Model layers were 1 ft thick. The vertical sequence of the model was composed of a 9 ft thick aquifer overlying a 1 ft thick low permeability unit. The use of the low permeability unit for the lowermost layer of the model improved the mass balance results. The overlying layers composing the aquifer were constructed using the following parameters: hydraulic conductivity, 3.0 ft/day; transmissivity, 27 ft^2/day; specific yield (Sy), 0.3; specific storage (Ss), 6E-6 $\frac{1}{ft}$; and effective porosity, 0.3. Well casing and screen radii were 0.3 ft and 0.25 ft, respectively. The pumping well was fully penetrating. The extraction rate was 20 ft^3/day for all simulations. The model boundaries were no-flow and the initial head was set at the upper surface of the model for all cells. The cell size was smallest in the region of the well increasing in size towards the model boundaries. Four models were created based on the smallest grid size of the model: 0.8 ft; 1.6 ft; 6.3 ft; and, 12.6 ft. Discretization for each model is shown in Table A-1. As the grid size increased moving outwards from the pumping well, the minimum and maximum grid size for each model is included in Table A-1. Models were run for 125 to 400 days and achieved successful mass balance results.

Minimum Grid Size (ft)	Maximum Grid Size (ft)	Duration (days)	% Mass Balance Discrepancy	Number of Rows	Number of Columns	Number of Layers
0.8	~ 1600	400	3.59	390	389	10
1.6	~ 800	125	5.59	161	143	10
6.3	~ 500	125	4.69	277	277	10
12.6	~ 500	125	4.77	246	245	10

Table A-1. Summary of the infinite areal extent verification models discretization.

Drawdown data was collected at the pumping well and imported into Aqtesolv for preparation and analysis of drawdown and derivative curves to assess predicted versus computed transmissivity and storage values. Type-curve matching to obtain the computed aquifer parameters was conducted using either the Neuman (1974) analytical solution for unconfined aquifers with instantaneous delayed gravity drainage or the Cooper-Jacob straight-line method (1946) with drawdown corrected for unconfined aquifers (Jacob 1944). The transmissivity value and specific yield values used by MODFLOW-SURFACT were 27 ft^2/day and 0.3, respectively. Aqtesolv provided an output of storativity denoted as "S". Storativity for an unconfined aquifer is the sum of specific yield and the product of specific storage (Ss) times the thickness of the aquifer (b):

$$S = Sy + (Ss \times b) \qquad \text{A (1)}$$

For the Neuman solution, storativity is the component under confined conditions or specific storage times the aquifer thickness. For the Cooper-Jacobs straight-line method, storativity is as shown in equation A(1). The value of S used in the MODFLOW-SURFACT data set was 5.4E-5 for the Neuman solution and 0.300054, or approximately 0.3 for the Cooper-Jacob method. Since output taken at the extraction well included wellbore storage effects, simulated storage values were anticipated to deviate from the predicted values. The drawdown curves and analyses are presented below. As the results slightly differ between the grids sizes, the 0.8 ft and 1.6 ft grids are discussed first with the 6.3 ft and 12.6 ft grids following.

The smaller grid sizes (0.8 ft and 1.6 ft) produced drawdown and derivative curves well matched to the respective type-curves (Figures A-1 and A-2). Table A-2

summarizes the simulated parameter results. The 0.8 ft grid was run for 400 days to clarify late time derivative curve undulations as likely forming from numerical issues. Therefore, at smaller grid sizes, the predicted and computed results for transmissivity were comparable.

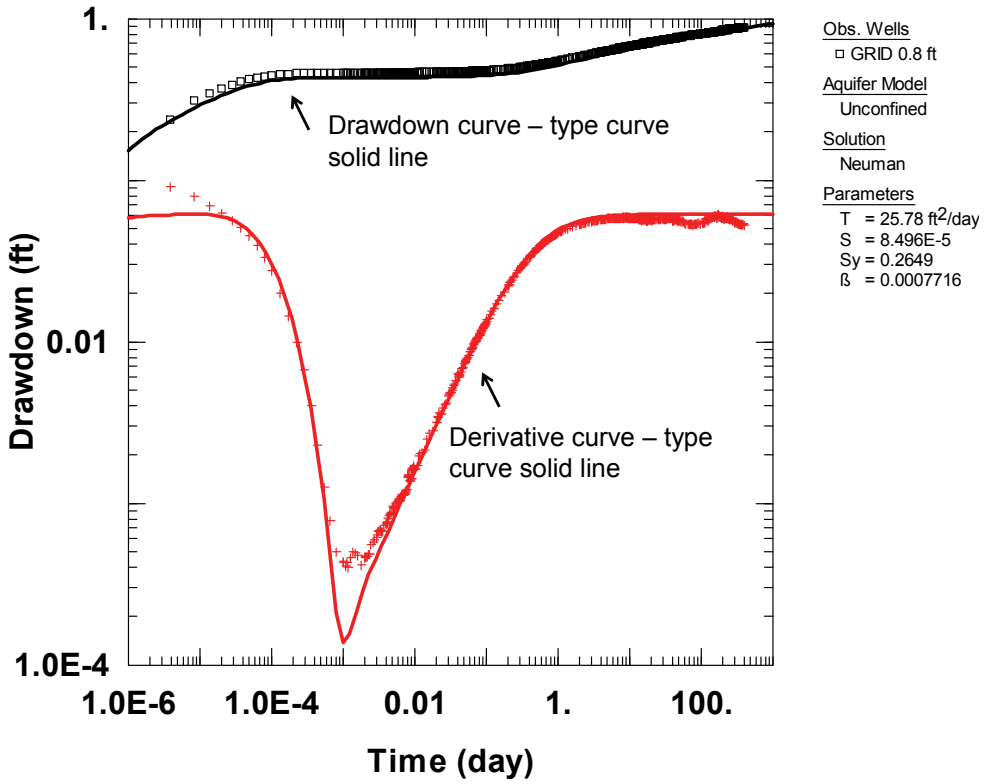

Figure A-1. Log-Log drawdown and derivative curves for the verification testing of a constant-rate pump test. Thin, solid lines denote type curves. Estimated parameter results using the Neuman (1974) solution for an unconfined aquifer are presented to the right of the time-drawdown plot. The simulated time-drawdown data was from the MODFLOW-SURFACT simulation using a grid size range of 0.8 ft at the well expanding to ~1600 ft at model boundaries.

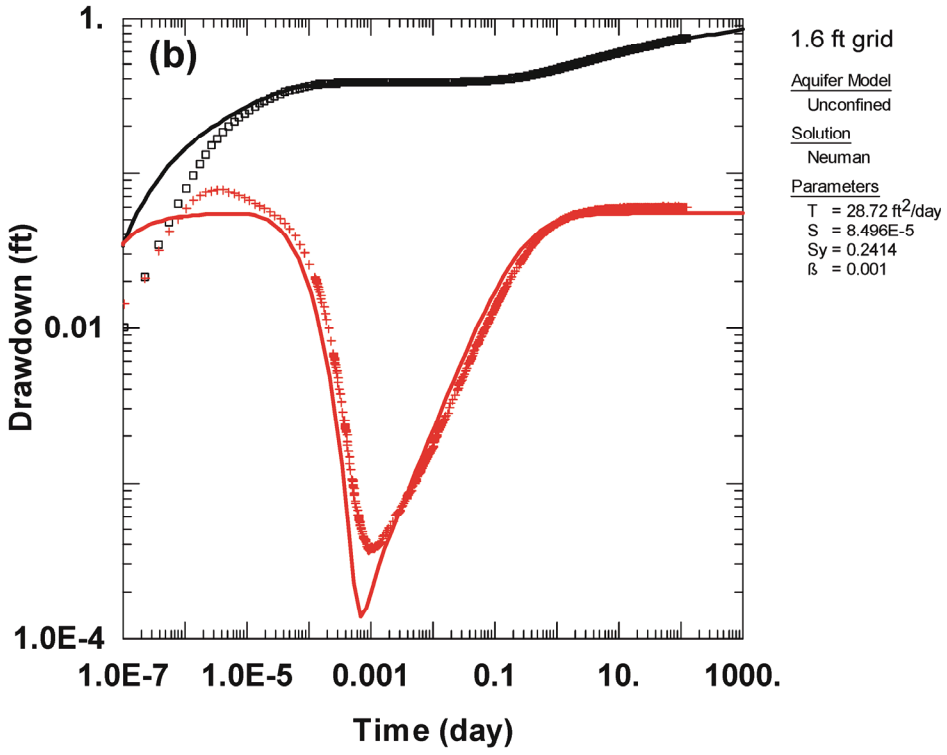

Figure A-2. Log-Log drawdown and derivative curves for the verification testing of a constant-rate pump test. Thin, solid lines denote type curves. Estimated parameter results using the Neuman (1974) solution for an unconfined aquifer are presented to the right of the time-drawdown plot. The simulated time-drawdown data was from the MODFLOW-SURFACT simulation using a grid size of 1.6 ft at the well expanding to ~800 ft at model boundaries.

Smallest Grid Size (ft)	Simulated T Value (ft^2/day)	Percent Discrepancy of Simulated T from Predicted Value of 27ft^2/day (%)	Simulated Sy Value	Percent Discrepancy of Simulated Sy from Predicted Value of 0.3 (%)	Simulated S (Ss *b)	Percent Discrepancy of Simulated S from Predicted Value of 5.4E-5 (%)
0.8 ft	25.78	4.5	0.2649	11.7	8.496E-5	57.3
1.6 ft	28.72	6.3	0.2414	19.5	8.496E-5	57.3

Table A-2. Summary of estimated parameter results for the finer grid models in the infinite areal extent verification models. Parameters estimated using the Neuman solution for an unconfined aquifer (1974). Abbreviations used: T is transmissivity, Sy is specific yield, Ss is specific storage, b is aquifer thickness, and S is storativity.

Figures A-3 and A-4 show the 6.3 and 12.6 ft grid tests. Separation is observed between the computed drawdown curve and the type-curves derived from input parameters. These type curves demonstrate the deviation of the computed response from the ideal type-curve response for the parameters used in the MODFLOW-SURFACT simulation. The larger grids also produced a compression of the delayed yield component followed by the development of a unit slope derivative curve into the late time interval. At larger grid sizes, curve matching using the Neuman solution was not effective. Given the poor results, the large grids were also analyzed using the Cooper-Jacob straight-line method (1946). Using the Jacob (1944) method, the drawdown was corrected for an unconfined aquifer. These analyses provided computed transmissivity values near predicted results for late time data (Table A-3). The increased grid size distorted the early and intermediate time results, with the late time curve response producing comparable

transmissivity values to that of a finer grid discretization. This implies the late time curve behavior was less sensitive to the larger grids (up to 10 and possibly 20 feet). The late time stability of the curve response suggests that the small variations in the grid size that were required to optimize the leaky perched aquifer simulations did not influence the late time curve behavior. This is important as the late time interval was the dominant period over which the simulations were analyzed. It should be noted that discrepancies persisted in storage values.

Grid	Simulated T Value (ft^2/day)	Percent Discrepancy of Simulated T from Predicted Value of 27ft^2/day (%)	Simulated S Value S= Sy+(Ss*b)	Percent Discrepancy of Simulated S from Predicted Value of ~ 0.3 (%)
6.3ft	28.21	4.48	4.835	~1400
12.6 ft	27.65	2.4	27.18	~9000

Table A-3. Summary of estimated parameter results for the larger grid models in the infinite areal extent verification models. Parameters estimated using the Cooper-Jacob straight-line method. Abbreviations used: Abbreviations used: T is transmissivity, Sy is specific yield, Ss is specific storage, b is aquifer thickness, and S is storativity.

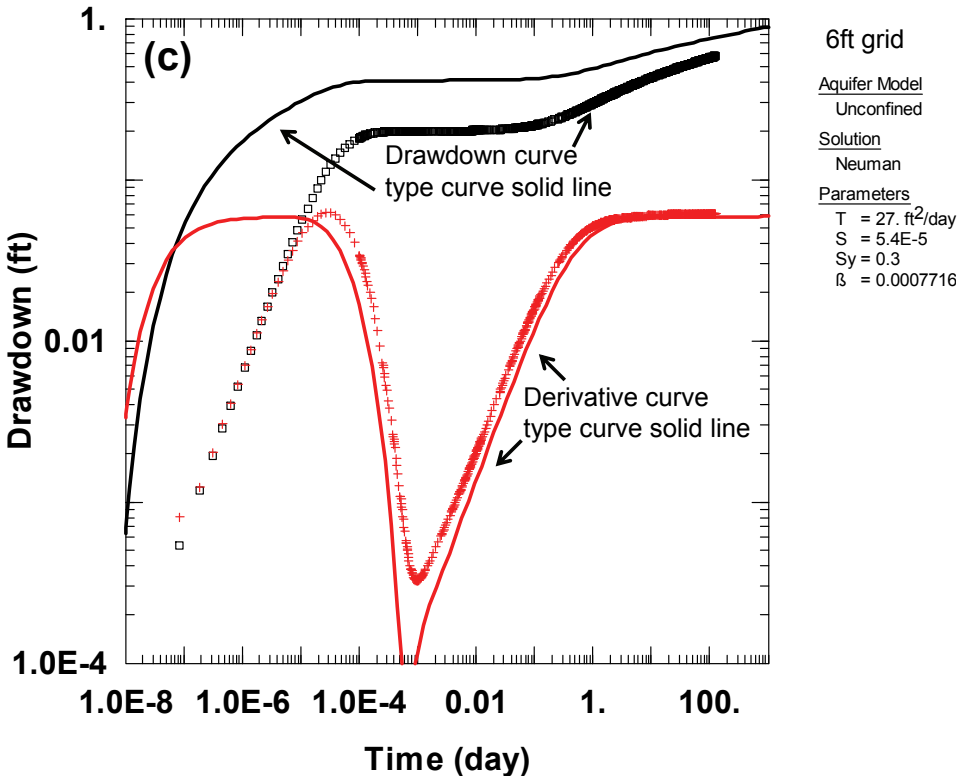

Figure A-3. Log-Log drawdown and derivative curves for the verification testing of a constant-rate pump test. Thin, solid lines are type curves corresponding to the predicted parameters presented to the right of the time-drawdown plot. The simulated time-drawdown data was from the MODFLOW-SURFACT simulation using a grid size of 6.3 ft at the well expanding to ~ 500 ft at the model boundaries.

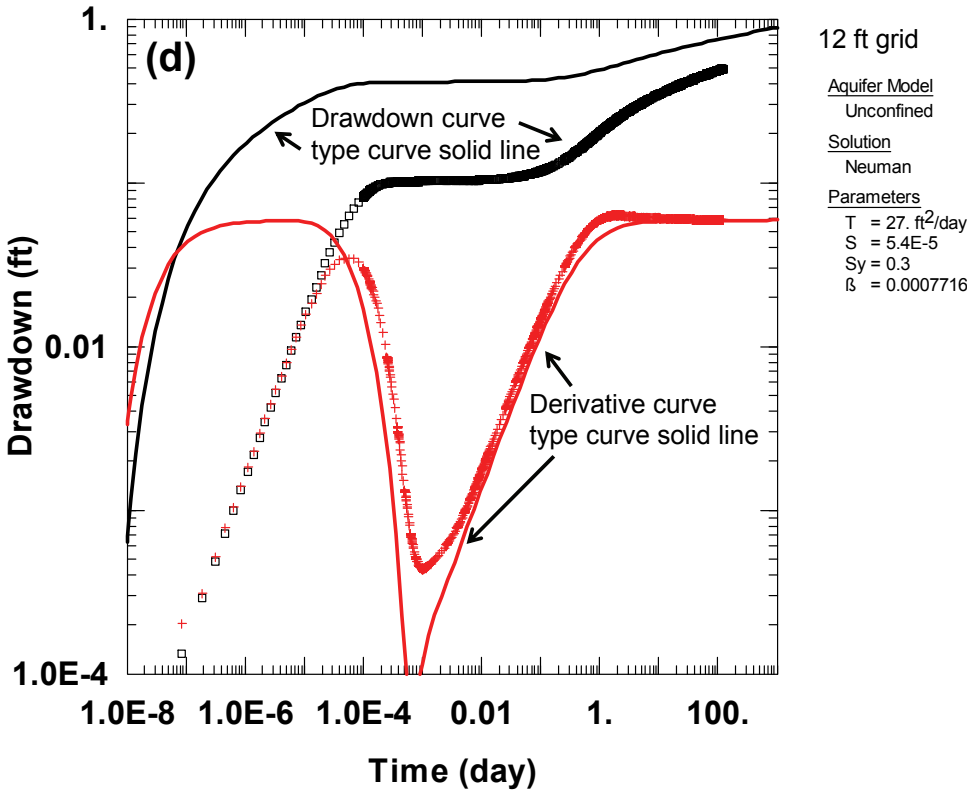

Figure A-4. Log-Log drawdown and derivative curves for the verification testing of a constant-rate pump test. Thin, solid lines are type curves corresponding to the predicted parameters presented to the right of the time-drawdown plot. The simulated time-drawdown data was form the MODFLOW-SURFACT simulation using a grid size of 12.6 ft at the well expanding to 500 ft at the model boundaries.

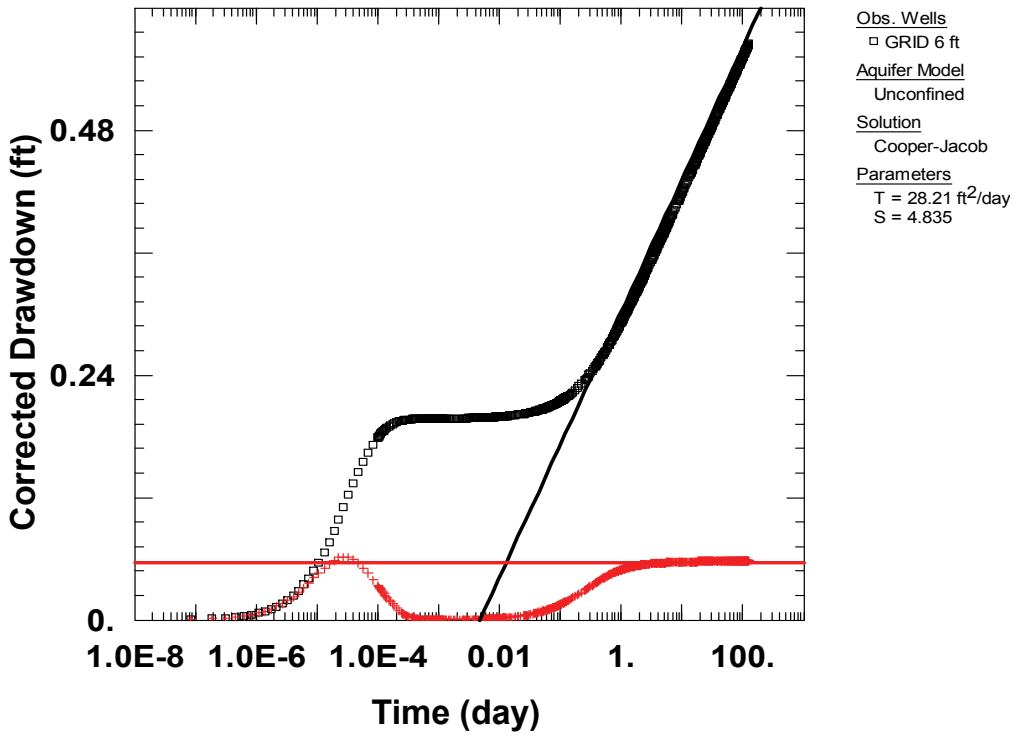

Figure A-5. Semilog drawdown and derivative curves for the verification testing of a constant-rate pump test. Analysis using Cooper- Jacob straight-line method. Thin, solid lines denote type curves. Estimated parameters are presented to the right of the time-drawdown plot. The simulated time-drawdown data was from the MODFLOW-SURFACT simulation using a grid size of 6.3 ft at the well expanding to ~ 500 ft at the model boundaries.

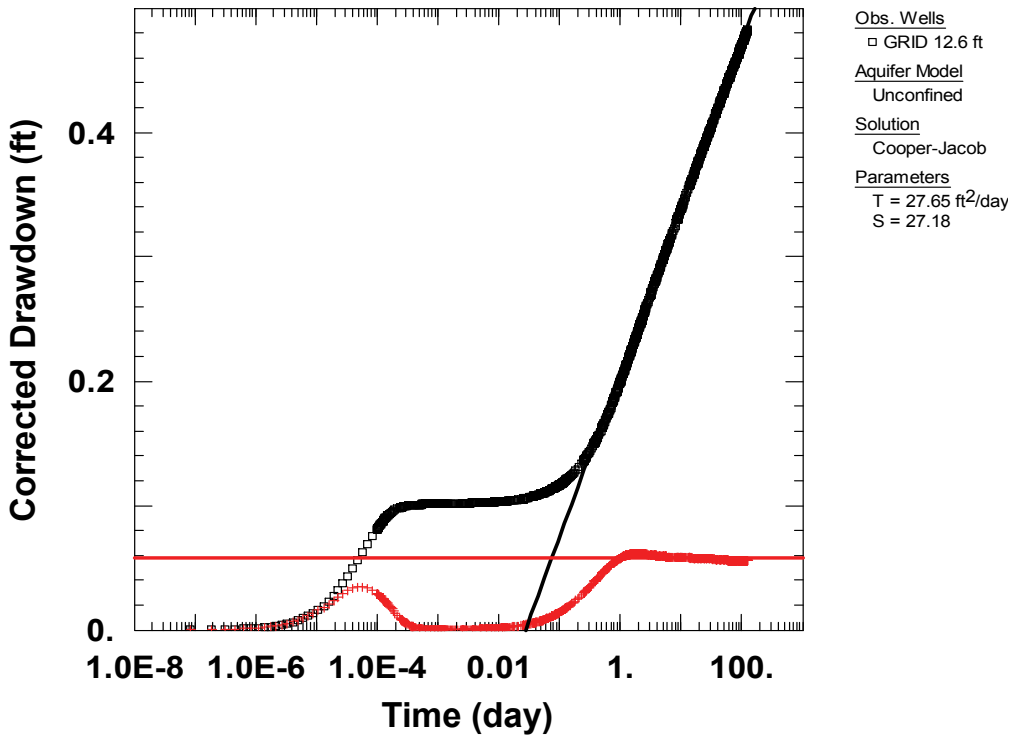

Figure A-6. Semilog drawdown and derivative curves for the verification testing of a constant-rate pump test. Analysis using Cooper- Jacob straight-line method. Thin, solid lines denote type curves. Estimated parameter results are presented to the right of the time-drawdown plot. The simulated time-drawdown data was form the MODFLOW-SURFACT simulation using a grid size of 12.6 ft at the well expanding to 500 ft at the model boundaries.

Limited-in-Extent Models

As perched aquifers are of limited areal extent, the ability of the software to capture drawdown patterns associated with boundaries was verified. Small models (100 ft (L) by 100 ft (W) by 20 ft (H)) were developed such that the model no-flow boundaries would be encountered during the pump test. Three models were used to test grid sizes of

0. 7 ft, 5 ft, and 10 ft on producing the anticipated drawdown and derivative curves. The 5 ft and 10 ft grid models had uniform grid spacing, while the 0.7 ft grid model utilized small grid spacing in the region of the well that became coarser moving towards the boundaries. Layer thicknesses were variable, ranging from 0.5 to 2 ft thick. The same aquifer parameters were used as for the infinite-in-extent models described above. The pumping rate was 200 ft^3/day for 125 days. Drawdown results were imported into Aqtesolv and are shown below.

Boundaries were observed in all models, as shown by the increase in drawdown and unit slope derivative at late time. In these small extent models, the no-flow boundaries surrounding the aquifer allow for the drainage of the system in an analogous manner to wellbore storage effects that produce a unit slope drawdown and derivative curve on the log-log plots. As shown by Renard et al. (2009), wellbore storage is comparable to a well drilled in an aquifer having zero transmissivity. The derivative curve and drawdown curve are of unit slope as:

$$s(t) = \frac{Q}{\pi r^2} t \qquad \text{(A-2)}$$

Where Q is pumping rate, t is time, r is radius of well casing, s is drawdown.
The derivative of drawdown with respect to the natural logarithm of time (ln t) is the derivative curve used in this study and is shown to equal the drawdown in the well as a function of time:

$$\frac{ds}{d\ln t} = t\frac{ds}{dt} = t\frac{Q}{\pi r^2} = s(t) \qquad \text{(A-3)}$$

Taking the logarithm of the above shows the derivative and the drawdown both equal to a line of unit slope when plotted on log-log scale with log [s(t)] on the y axis and log(t) on the x axis:

$$\log[s(t)] = \log[\frac{ds}{d\ln t}] = \log(t) + \log[\frac{Q}{\pi r^2}] \qquad \text{(A-4)}$$

The limited-in-extent models behave in a similar manner to the wellbore storage described above with the casing radius analogous to the distance to the model boundaries, draining in a comparable pattern.

The results indicate the variation in the grid sizes did not influence the appearance of the boundary effect.

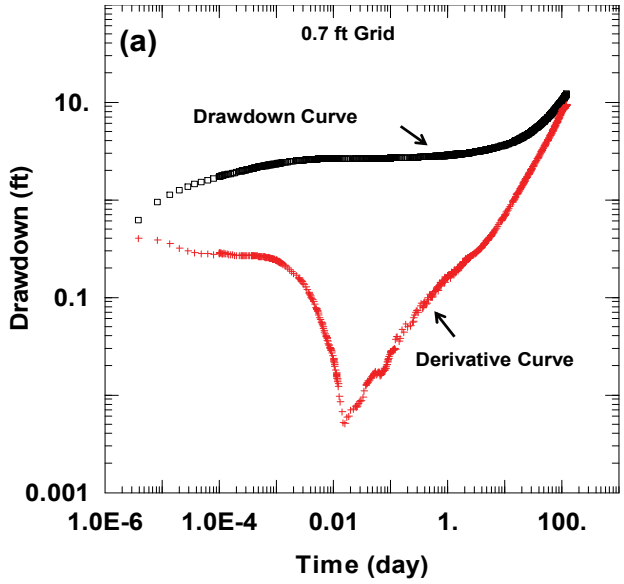

Figure A-5. Log-Log drawdown and derivative curves for verification testing of curve response to encountering model no-flow boundaries. The MODFLOW-SURFACT grid varied between 0.7 ft at the well expanding to 5.0 ft at the model boundaries.

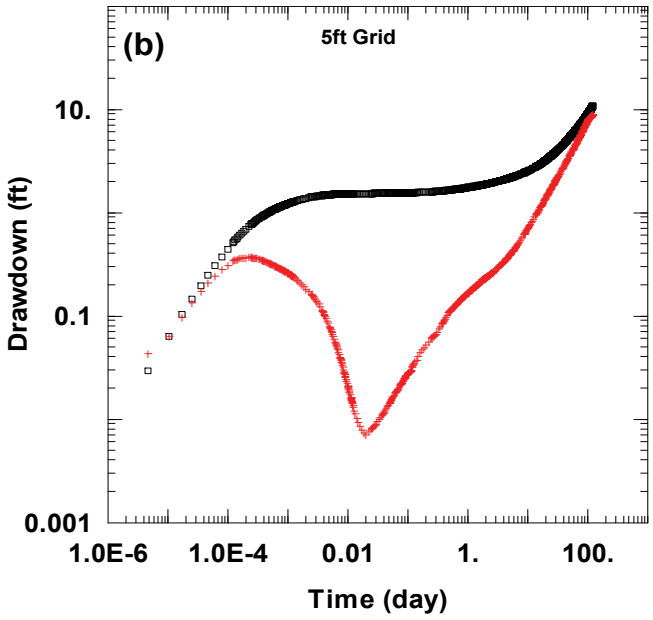

Figure A-6. Log-Log drawdown and derivative curves for verification testing of curve response to encountering model no-flow boundaries, 5 ft grid.

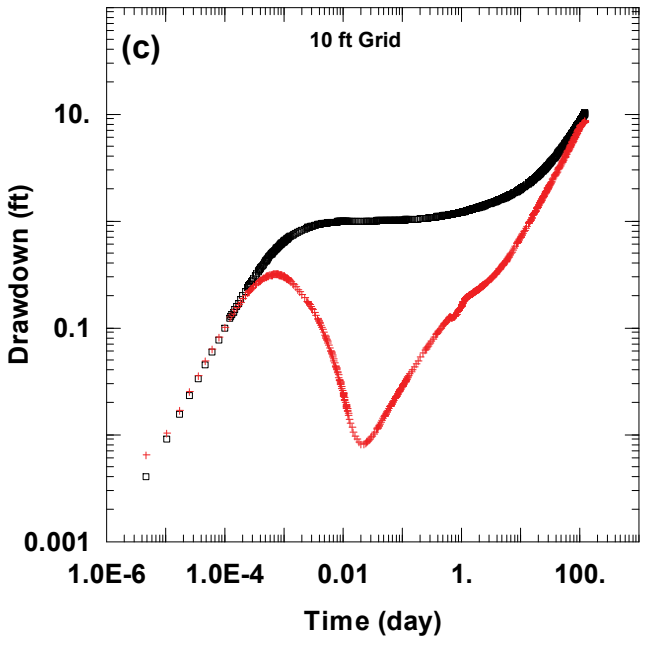

Figure A-7. Log-Log drawdown and derivative curves for verification testing of curve response to encountering model no-flow boundaries, 10 ft grid.

APPENDIX B - ADDITIONAL MODELS

Results from the leaky perched aquifer simulations conducted at high pump rates show a positive slope-derivative curve. While the appearance of a positive slope-derivative suggests boundary influences, observations during this study indicated a reducing transmissivity could also contribute to a positive slope-derivative curve. Low transmissivity and high pump rates each lead to a deepening of the cone of depression at the wellbore (Hall 1996). This implies that a thin, low permeable aquifer subjected to high pumping rates will experience a decreasing transmissivity as the aquifer height is lowered in the region of the well, and therefore, an increase in drawdown. To determine the influence of reduced transmissivity at the wellbore, constant-rate pump tests were simulated in a thin, infinite-in-extent, unconfined aquifer. The model was 100,000 ft (L) by 100,000 ft (W) by 10 ft (H) with parameters the same as the circular leaky perched aquifer, 3.0 ft/day hydraulic conductivity model. Grid size was refined at the pumping well. A series of three models were developed, defined by the smallest grid spacing: 4 ft; 6 ft; and 12 ft. The grid size increased outwards to a maximum grid size of 500 ft for all models. Testing various grid sizes was conducted as issues of dewatering can arise from numerical limitations when a high pumping rate in a low transmissivity unit is unable to extract sufficient water over the time step. Increasing the grid size was found to alleviate the dewatering. Therefore, testing of differing grid sizes was included to ensure that the

development of a positive slope-derivative curve was not the product of a tight grid size. The models were run at pump rates 200 ft^3/day. The infinite-in-extent model sequence produced a slightly positive slope-derivative curve for all grid sizes (a slope of approximately 0.15). A lower pump rate test of 20 ft^3/day was conducted using the 6 ft grid for comparison. The low pump rate showed a horizontal derivative indicative of radial flow (Renard et al. 2009). Boundaries were not encountered in any simulation, suggesting the positive slope-derivative curve resulted from a higher pumping rate that induced an increasing rate of drawdown to meet well demands. The results of the pump tests demonstrate the ability to produce a positive slope-derivative curve from a reduced transmissivity at the wellbore, a product of the reduced thickness as water was removed from storage to meet the higher pump demands.

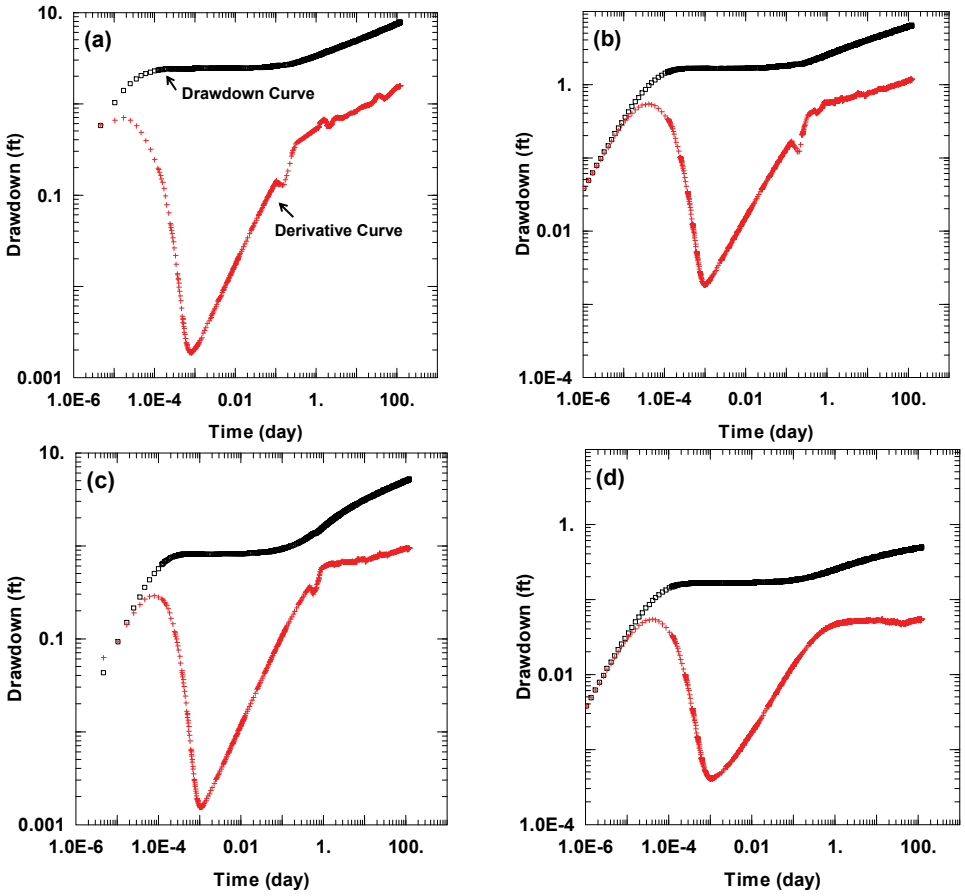

Figure B-5. Log-Log drawdown and derivative curves for the unconfined, infinite in areal extent models 200 ft^3/day pumping-rate tests with a grid spacing of (a) 4 ft, (b) 6 ft and (c) 12 ft. The 20 ft^3/day pumping-rate test with a grid spacing of 6 ft is shown in (d).